Current-density implementation for calculating flexoelectric coefficients

Cyrus E. Dreyer,[1] Massimiliano Stengel,[2,3] and David Vanderbilt[1]

[1] *Department of Physics and Astronomy, Rutgers University, Piscataway, New Jersey 08845-0849, USA*
[2] *ICREA-Institució Catalana de Recerca i Estudis Avançats, 08010 Barcelona, Spain*
[3] *Institut de Ciència de Materials de Barcelona (ICMAB-CSIC), Campus UAB, 08193 Bellaterra, Spain*

(Dated: February 20, 2018)

The flexoelectric effect refers to polarization induced in an insulator when a strain gradient is applied. We have developed a first-principles methodology based on density-functional perturbation theory to calculate the elements of the bulk, clamped-ion flexoelectric tensor. In order to determine the transverse and shear components directly from a unit cell calculation, we calculate the current density induced by the adiabatic atomic displacements of a long-wavelength acoustic phonon. Previous implementations based on the charge-density response required supercells to capture these components. Our density-functional-theory implementation requires the development of an expression for the current density that is valid for the case of nonlocal pseudopotentials, and long-wavelength phonon perturbations. We benchmark our methodology on simple systems of isolated noble gas atoms, and apply it to calculate the clamped-ion flexoelectric constants for a variety of technologically important cubic oxides. We also discuss some technical issues that are associated with the definition of current density in a nonlocal pseudopotential context, and their relevance to the calculation of macroscopic response properties of crystals.

I. INTRODUCTION

The flexoelectric (FxE) effect, where polarization is induced by a strain gradient, is universal in all insulators. As devices shrink to the micro and nano scale, large strain gradients can occur, and therefore the FxE effect can play a significant role in the properties of such devices, influencing the so-called dielectric dead layer,[1] domain walls and domain structure,[2–4] relative permittivity and Curie temperature,[5,6] critical thickness of films to exhibit switchable polarization,[7] and spontaneous polarization in the vicinity of twin and antiphase boundaries.[8] Also, the FxE effect can be exploited for novel device design paradigms, such as piezoelectric "meta-materials" constructed from nonpiezoelectric constituents,[9,10] or mechanical switching of ferroelectric polarization.[11,12]

One of the crucial limitations to understanding and exploiting the FxE effect is the lack of a clear experimental and theoretical consensus on the size and sign of the FxE coefficients, even in commonly studied materials such at $SrTiO_3$ and $BaTiO_3$.[13,14] A key element to forming this understanding is the development of an efficient first-principles methodology to calculate all of the components of the bulk FxE tensor. Recently, Stengel,[15] and Hong and Vanderbilt[16,17] (HV), developed the formalism for calculating the full bulk FxE tensor from first principles.

The implementation[16,17] of the HV methodology involved using density functional theory (DFT) to calculate the real space charge-density response to displacements of atoms in a supercell of bulk material. This allowed access to the longitudinal bulk FxE coefficients. In the implementation[18] of Stengel's methodology, the charge-density response to a long-wavelength acoustic phonon was calculated. This allowed the longitudinal FxE coefficients to be determined from a unit cell linear-response calculation using density-functional perturbation theory (DFPT).[19] In order to calculate the transverse and shear FxE coefficients, Stengel related them to the open circuit field across a slab perturbed by a long wavelength acoustic phonon; therefore this implementation required DFPT calculations to be performed on a slab supercell.

The reliance on computationally intensive supercell and slab calculations represents significant limitation to efficient calculation of FxE coefficients on a wide variety of materials. Therefore, it is desirable to develop a methodology to obtain the full bulk FxE tensor (longitudinal, transverse, and shear components) from calculations on single unit cell. This poses a major technical challenge in the context of DFPT. Indeed, the transverse and shear components are, in principle, not obtainable from the induced charge density in bulk; this is a result of the fact that the charge density is given by the divergence of the polarization. It is required that the induced polarization response be calculated, which is related to the *current* density.[15,17,20] Therefore, a methodology must be implemented to calculate the current density induced by a strain gradient perturbation.[15,17,20] This is trickier than it sounds: since the strain gradient breaks the periodicity of the lattice, the *microscopic* current density response to a strain gradient is required. Therefore, the now widespread treatment based on the Berry-phase formulation[21,22] is not sufficient since it only provides the macroscopic response.

This, in principle, does not appear as an overly serious issue: The microscopic current density is a fundamental quantum-mechanical observable, whose expression is well known.[23] The textbook formula for the probability current, however, is problematic if the Hamiltonian of interest contains *nonlocal* potentials, as it no longer satisfies the continuity equation,[24] and therefore is unfit as a basis for the current-response theory we have in mind (we expand on this in Sec. III B). This issue is very relevant in the context of DFT. Most popular implementations

rely on a basis set of plane waves to expand the single-particle wavefunctions, and, in order to reduce the size of the basis set necessary, core electrons are described with pseudopotentials. Modern pseudopotential implementations contain nonlocal potentials in the form of projectors that operate on the wavefunctions.[25–28]

The definition and calculation of the microscopic current density in a nonlocal pseudopotential context is a rather general problem that has received considerable previous attention[24,29–34] in view of its application to the calculation of magnetic susceptibility,[30–34] nuclear magnetic resonance chemical shifts,[35] electron paramagnetic resonance g tensors,[36] and so forth. Unfortunately a general, systematic solution that is appropriate to our scopes has not emerged yet. To see why this is challenging, it is important to note that the continuity equation is only one of the criteria that must be satisfied by a physically meaningful definition of the current density. Two other criteria are important. First, the formula must also reduce to the textbook expression in regions of space that lie outside the range of the nonlocal operators (pseudopotentials are typically confined to small spheres surrounding the atoms). Second, it must reduce to the well-known expressions for the macroscopic current in the long-wavelength limit. The approaches that have been proposed so far have either been specialized to a certain physical property (e.g., dielectric[29] or diamagnetic[32] response), or limited in scope to a subset of the above criteria. For example, Li *et al.*[24] proposed a strategy that guarantees charge continuity by construction but does not satisfy the two additional criteria, as we shall see in Sec. III B.

In this work we develop a first-principles methodology based on DFT to calculate the full bulk, clamped-ion FxE tensor from a single unit cell. At the heart of our technique lies the introduction of a physically sound current-density operator in presence of nonlocal pseudopotentials, which we define as the linear coupling of the Hamiltonian to an external vector potential field.

We show that such definition fulfills all criteria that we stated in the above paragraphs: (i) it satisfies the continuity equation; (ii) the contribution of the nonlocal pseudopotentials is correctly confined to the atomic spheres; and (iii) it reduces to the macroscopic velocity operator in the long-wavelength limit. We will discuss our approach for calculating the current density in the context of earlier works, and how it applies to the problem of calculating bulk FxE coefficients.

The paper is organized as follows. In Sec. II we outline the general approach to determining FxE coefficients; in Sec. III we give the formalism used in our calculations of the current density; in Sec. IV we provide details of the implementation of the formalism; Sec. V presents benchmark tests for the simple case of isolated noble gas atoms, and results for several technologically important, cubic oxide compounds; in Sec. VI, we discuss some technical issues that are associated with the current density in the presence of nonlocal pseudopotentials; we conclude the paper in Sec. VII.

II. APPROACH

The goal of this work is to calculate the bulk clamped-ion flexoelectric tensor elements

$$\mu^{\mathrm{I}}_{\alpha\beta,\omega\nu} = \frac{dP_\alpha}{d\eta_{\beta,\omega\nu}}, \tag{1}$$

where P_α is the polarization in direction α, and

$$\eta_{\beta,\omega\nu} = \frac{\partial^2 u_\beta}{\partial r_\omega \partial r_\nu} \tag{2}$$

is the strain gradient tensor, where u_β is the β component of the displacement field. The superscript "I" indicates that the tensor elements are defined with respect to the unsymmetrized displacements;[37] superscripts "II" will be used to indicate tensor elements defined with respect to symmetrized strain.

Calculating the polarization in Eq. (1) is tricky from a quantum-mechanical standpoint, as it does not correspond to the expectation value of a well-defined operator. Moreover, we will need access to the local polarization density $P_\alpha(\mathbf{r})$, so Berry-phase methods are not applicable.

At the linear-response level the induced polarization $P_{\alpha,\lambda}(\mathbf{r}) = \partial P_\alpha(\mathbf{r})/\partial\lambda$ resulting from a small change in parameter λ can be equated to the local current flow via $\partial P_\alpha(\mathbf{r})/\partial\lambda = \partial J_\alpha(\mathbf{r})/\partial\dot{\lambda}$, where $\dot{\lambda}$ is the rate of change of adiabatic parameter λ. Following the approach of Ref. 15, we now consider an adiabatic displacement of sublattice κ of a crystal in direction β as given by

$$u_{\kappa\beta}(l,t) = \lambda_{\kappa\beta\mathbf{q}}(t) e^{i\mathbf{q}\cdot\mathbf{R}_{l\kappa}} \tag{3}$$

where l is the cell index. In this case the induced local polarization density $P_{\alpha,\kappa\beta\mathbf{q}}(\mathbf{r})$ in direction α induced by mode $\kappa\beta$ of wavevector $\mathbf{q}$ is

$$P_{\alpha,\kappa\beta\mathbf{q}}(\mathbf{r}) = \frac{\partial J_\alpha(\mathbf{r})}{\partial\dot{\lambda}_{\kappa\beta\mathbf{q}}}. \tag{4}$$

Using the fact that the linearly induced current will be modulated by a phase with the same wavevector as the perturbation in Eq. (3), we can define

$$P^{\mathbf{q}}_{\alpha,\kappa\beta}(\mathbf{r}) = P_{\alpha,\kappa\beta\mathbf{q}}(\mathbf{r}) e^{-i\mathbf{q}\cdot\mathbf{r}}, \tag{5}$$

which is therefore a lattice-periodic function. This quantity, the *cell-periodic part of the first-order induced polarization density*, will play a central role in our considerations. It is also convenient to define

$$\overline{P}^{\mathbf{q}}_{\alpha,\kappa\beta} \equiv \frac{1}{\Omega}\int_{\mathrm{cell}} P^{\mathbf{q}}_{\alpha,\kappa\beta}(\mathbf{r}) d^3r, \tag{6}$$

where Ω is the cell volume, as the cell average of this response. In Ref. 15 it was shown that the clamped-ion flexoelectric tensor elements are given by the second wavevector derivatives of $\overline{P}^{\mathbf{q}}_{\alpha,\kappa\beta}$ via

$$\mu^{\mathrm{I}}_{\alpha\beta,\omega\nu} = -\frac{1}{2}\sum_{\kappa}\left.\frac{\partial^2 \overline{P}^{\mathbf{q}}_{\alpha,\kappa\beta}}{\partial q_\omega \partial q_\nu}\right|_{\mathbf{q}=0}. \tag{7}$$

This formulation suggests that it may be possible to compute the polarization responses $\overline{P}^{\mathbf{q}}_{\alpha,\kappa\beta}$ entirely from a single-unit-cell calculation, similar to the way that phonon responses are computed in DFPT. In fact, this is the case. The formalism necessary to compute these responses at the DFT level will be presented in the next sections, giving access to an efficient and robust means to compute the flexoelectric coefficients through Eq. (7).

III. FORMALISM

Given a time-dependent Hamiltonian with a single-particle solution $\Psi(t)$, the current density at a point $\mathbf{r}$ in Cartesian direction α can be written

$$J_\alpha(\mathbf{r}) = \langle\Psi(t)|\hat{\mathcal{J}}_\alpha(\mathbf{r})|\Psi(t)\rangle \tag{8}$$

where $\hat{\mathcal{J}}_\alpha(\mathbf{r})$ is the current-density operator (a caret symbol over a quantity will indicate an operator). We will first address how to treat the time-dependent wavefunctions (Sec. III A), and then discuss the form of the current-density operator in (Sec. III B) .

A. Adiabatic density-functional perturbation theory

1. Adiabatic response

We write the time-dependent Shrödinger equation as

$$i\frac{\partial}{\partial t}|\Psi\rangle = \hat{H}(\lambda(t))|\Psi\rangle. \tag{9}$$

where $\hat{H}(\lambda(t))$ is the Hamiltonian, and λ parametrizes the time-dependent atomic motion. Since we are interested in the current density resulting from adiabatic displacements, we expand the wavefunction $\Psi(t)$ to first order in the velocity, $\dot{\lambda}$:[38–40]

$$\Psi(t) \simeq e^{i\gamma(t)}e^{i\phi(\lambda(t))}[|\psi(\lambda(t))\rangle + \dot{\lambda}(t)|\delta\psi(\lambda(t))\rangle], \tag{10}$$

where $\psi(\lambda)$ is the lowest-energy eigenfunction of the time-independent Hamiltonian at a given λ; $\gamma(t) = -\int_0^t E(\lambda(t'))dt'$ is the dynamic phase; $\phi(\lambda(t)) = \int_0^t \langle\psi(\lambda(t'))|i\partial_t\psi(\lambda(t'))\rangle dt'$ is the geometric Berry phase[41] (we have used the shorthand $\partial_t = \partial/\partial t$). We work in the parallel-transport gauge, $\langle\psi(\lambda)|i\partial_\lambda\psi(\lambda)\rangle = 0$, so the Berry phase contribution vanishes.

Equation (10) is written assuming a single occupied band, but in the multiband case we shall let the evolution be guided by multiband parallel transport instead. In this case, the first-order wavefunctions, $\delta\psi_n$, given by adiabatic perturbation theory,[38–40] are

$$|\delta\psi_n\rangle = -i\sum_{m}^{\mathrm{unocc}}|\psi_m\rangle\frac{\langle\psi_m|\partial_\lambda\psi_n\rangle}{\epsilon_n - \epsilon_m}, \tag{11}$$

where ϵ_n is the eigenvalue of the nth single particle wavefunctions, and ∂_λ is shorthand for $\partial/\partial\lambda$. The wavefunction $|\partial_\lambda\psi_n\rangle$ is the first-order wavefunction resulting from the *static* perturbation:

$$|\partial_\lambda\psi_n\rangle = \sum_{m}^{\mathrm{unocc}}|\psi_m\rangle\frac{\langle\psi_m|\partial_\lambda\hat{H}|\psi_n\rangle}{\epsilon_n - \epsilon_m}, \tag{12}$$

which is the quantity calculated in conventional DFPT implementations.[19,42]

2. Density functional theory

We will implement the calculations of the current density in the context of plane-wave pseudopotential DFT, so the single-particle wavefunctions we will use in Eq. (11) are solutions to the Kohn-Sham equation for a given band n and wavevector $\mathbf{k}$,

$$\hat{H}_{\mathrm{KS}}|\psi_{n\mathbf{k}}\rangle = \epsilon_{n\mathbf{k}}|\psi_{n\mathbf{k}}\rangle. \tag{13}$$

where the Kohn-Sham Hamiltonian is

$$\hat{H}_{\mathrm{KS}} = \hat{T}_{\mathrm{s}} + \hat{V}_{\mathrm{H}} + \hat{V}_{\mathrm{XC}} + \hat{V}^{\mathrm{loc}}_{\mathrm{ext}} + \hat{V}^{\mathrm{nl}}_{\mathrm{ext}}. \tag{14}$$

Here $\hat{T}_{\mathrm{s}}$ is the single-particle kinetic energy, $\hat{V}_{\mathrm{H}}$ is the Hartree potential, $\hat{V}_{\mathrm{XC}}$ is the exchange correlation potential, and the external potential contains both a local and nonlocal part (last two terms). We will consider norm-conserving, separable, Kleinmann-Bylander type[27] pseudopotentials. The form of the nonlocal potential (henceforth referred to as $\hat{V}^{\mathrm{nl}}$) is given by Eq. (C1). We will drop the "KS" subscript from here on.

3. Polarization response

Using the expansion in Eq. (10), the first-order one-particle density matrix is

$$\delta\hat{\rho} = \dot{\lambda}\frac{2}{N_k}\sum_{n\mathbf{k}}\left(|\delta\psi_{n\mathbf{k}}\rangle\langle\psi_{n\mathbf{k}}| + |\psi_{n\mathbf{k}}\rangle\langle\delta\psi_{n\mathbf{k}}|\right) \tag{15}$$

where the factors $(2/N_k)\sum_{n\mathbf{k}}$ take care of the spin degeneracy, sum over occupied Bloch bands, and average over the Brillouin zone. A monochromatic perturbation such as that of Eq. (3) always comes together with its Hermitian conjugate, coupling states at $\mathbf{k}$ with those at $\mathbf{k}\pm\mathbf{q}$,

so that each perturbed wavefunction has two components that we refer as $\delta\psi_{n,\mathbf{k}+\mathbf{q}}$ and $\delta\psi_{n,\mathbf{k}-\mathbf{q}}$ respectively. We wish to select the cross-gap response at $+\mathbf{q}$, so we project onto this component of the density matrix to obtain[43]

$$\delta\hat{\rho}_{\mathbf{q}} = \dot{\lambda}\frac{2}{N_k}\sum_{n\mathbf{k}}\left(|\delta\psi_{n,\mathbf{k}+\mathbf{q}}\rangle\langle\psi_{n\mathbf{k}}| + |\psi_{n\mathbf{k}}\rangle\langle\delta\psi_{n,\mathbf{k}-\mathbf{q}}|\right). \tag{16}$$

Specializing now to the perturbation of Eq. (3), the corresponding polarization response is

$$P_{\alpha,\kappa\beta\mathbf{q}}(\mathbf{r}) = \frac{2}{N_k}\sum_{n\mathbf{k}}\Big[\langle\psi_{n\mathbf{k}}|\hat{\mathcal{J}}_\alpha(\mathbf{r})|\delta\psi^{\kappa\beta}_{n\mathbf{k},\mathbf{q}}\rangle + \langle\delta\psi^{\kappa\beta}_{n\mathbf{k},-\mathbf{q}}|\hat{\mathcal{J}}_\alpha(\mathbf{r})|\psi_{n\mathbf{k}}\rangle\Big]. \tag{17}$$

Using Eqs. (11) and (12), the needed first-order wave functions are

$$|\delta\psi^{\kappa\beta}_{n\mathbf{k},\mathbf{q}}\rangle = -i\sum_{m}^{\text{unocc}}|\psi_{m\mathbf{k}+\mathbf{q}}\rangle\frac{\langle\psi_{m\mathbf{k}+\mathbf{q}}|\partial_{\lambda_{\kappa\beta\mathbf{q}}}\hat{H}|\psi_{n\mathbf{k}}\rangle}{(\epsilon_{m\mathbf{k}+\mathbf{q}}-\epsilon_{n\mathbf{k}})^2}. \tag{18}$$

For Eq. (7), we require the cell-average of the $\mathbf{q}$-dependent polarization response,

$$\overline{P}^{\mathbf{q}}_{\alpha,\kappa\beta} = \frac{1}{\Omega}\int_{\text{cell}} d^3r\, e^{-i\mathbf{q}\cdot\mathbf{r}}\, P_{\alpha,\kappa\beta\mathbf{q}}(\mathbf{r}). \tag{19}$$

Defining the operator

$$\hat{\mathcal{J}}_\alpha(\mathbf{q}) = \frac{1}{\Omega}\int_{\text{cell}} d^3r\, e^{-i\mathbf{q}\cdot\mathbf{r}}\,\hat{\mathcal{J}}_\alpha(\mathbf{r}), \tag{20}$$

Eq. (19) can be written

$$\overline{P}^{\mathbf{q}}_{\alpha,\kappa\beta} = \frac{2}{N_k}\sum_{n\mathbf{k}}\Big[\langle\psi_{n\mathbf{k}}|\hat{\mathcal{J}}_\alpha(\mathbf{q})|\delta\psi^{\kappa\beta}_{n\mathbf{k},\mathbf{q}}\rangle + \langle\delta\psi^{\kappa\beta}_{n\mathbf{k},-\mathbf{q}}|\hat{\mathcal{J}}_\alpha(\mathbf{q})|\psi_{n\mathbf{k}}\rangle\Big]. \tag{21}$$

The ground-state and first-order wavefunctions can be expressed in terms of cell-periodic Bloch functions in the normal way

$$\langle\mathbf{s}|\psi_{n\mathbf{k}}\rangle = u_{n\mathbf{k}}(\mathbf{s})e^{i\mathbf{k}\cdot\mathbf{s}},\;\; \langle\mathbf{s}|\delta\psi^{\kappa\beta}_{n\mathbf{k},\mathbf{q}}\rangle = \delta u^{\kappa\beta}_{n\mathbf{k},\mathbf{q}}(\mathbf{s})e^{i(\mathbf{k}+\mathbf{q})\cdot\mathbf{s}} \tag{22}$$

(Indices $\mathbf{s}$ and $\mathbf{s}'$ are not to be confused with the point $\mathbf{r}$ at which the current density is evaluated.) Using this notation, the cell-periodic first-order static wavefunction is written $|\partial_\lambda u^{\kappa\beta}_{n\mathbf{k},\mathbf{q}}\rangle$, which is equivalent to $|u^{\tau_{\kappa\beta}}_{n\mathbf{k},\mathbf{q}}\rangle$ in the notation of Gonze and Lee[42] and $|\Delta u^{\mathbf{k}+\mathbf{q}}_n\rangle$ in the notation of Baroni *et al.*[19]

By factoring out the phases with wavevector $\mathbf{k}$ and $\mathbf{q}$, we can insure that we only consider cell-periodic quantities, and therefore all calculations can be performed on a unit cell.[19] To this end, we define a cell-periodic operator[44]

$$\hat{\mathcal{J}}^{\mathbf{k},\mathbf{q}}_\alpha = e^{-i\mathbf{k}\cdot\hat{\mathbf{r}}}\hat{\mathcal{J}}_\alpha(\mathbf{q})e^{i(\mathbf{k}+\mathbf{q})\cdot\hat{\mathbf{r}}}. \tag{23}$$

Using the fact that $\hat{\mathcal{J}}_\alpha(\mathbf{q}) = \hat{\mathcal{J}}^\dagger_\alpha(-\mathbf{q})$ it follows that $\left(\hat{\mathcal{J}}^{\mathbf{k},-\mathbf{q}}_\alpha\right)^\dagger = e^{-i(\mathbf{k}-\mathbf{q})\cdot\hat{\mathbf{r}}}\hat{\mathcal{J}}_\alpha(\mathbf{q})e^{i\mathbf{k}\cdot\hat{\mathbf{r}}}$ so that Eq. (21) can be written as

$$\overline{P}^{\mathbf{q}}_{\alpha,\kappa\beta} = \frac{2}{N_k}\sum_{n\mathbf{k}}\Big[\langle u_{n\mathbf{k}}|\hat{\mathcal{J}}^{\mathbf{k},\mathbf{q}}_\alpha|\delta u^{\kappa\beta}_{n\mathbf{k},\mathbf{q}}\rangle + \langle\delta u^{\kappa\beta}_{n\mathbf{k},-\mathbf{q}}|\left(\hat{\mathcal{J}}^{\mathbf{k},-\mathbf{q}}_\alpha\right)^\dagger|u_{n\mathbf{k}}\rangle\Big]. \tag{24}$$

In this work we shall limit our focus to materials with time-reversal symmetry (TRS); then we have

$$\langle\mathbf{s}|u_{n\mathbf{k}}\rangle = \langle u_{n-\mathbf{k}}|\mathbf{s}\rangle,\;\; \langle\mathbf{s}|\delta u^{\kappa\beta}_{n\mathbf{k},\mathbf{q}}\rangle = -\langle\delta u^{\kappa\beta}_{n\,-\mathbf{k},-\mathbf{q}}|\mathbf{s}\rangle, \tag{25}$$

where the negative sign in the second expression is a result of the $-i$ in the first-order adiabatic wavefunction [see Eq. (11)]. Assuming that the current operator has the correct "TRS odd" nature, i.e., $\left(\langle\mathbf{s}|\hat{\mathcal{J}}^{\mathbf{k},-\mathbf{q}}_\alpha|\mathbf{s}'\rangle\right)^* = -\langle\mathbf{s}|\hat{\mathcal{J}}^{-\mathbf{k},\mathbf{q}}_\alpha|\mathbf{s}'\rangle$, Eq. (24) simplifies to

$$\overline{P}^{\mathbf{q}}_{\alpha,\kappa\beta} = \frac{4}{N_k}\sum_{n\mathbf{k}}\langle u_{n\mathbf{k}}|\hat{\mathcal{J}}^{\mathbf{k},\mathbf{q}}_\alpha|\delta u^{\kappa\beta}_{n\mathbf{k},\mathbf{q}}\rangle. \tag{26}$$

B. Current-density operator

1. *Local potentials*

We now consider the form of the current-density operator. In the textbook derivation, current density is defined via the continuity condition

$$\nabla\cdot\mathbf{J}(\mathbf{r}) = -\frac{\partial\rho(\mathbf{r})}{\partial t}, \tag{27}$$

where ρ is the particle density, which is a conserved quantity. In a quantum mechanical treatment,[23] $\rho(\mathbf{r}) = |\Psi(\mathbf{r})|^2$, where Ψ is the solution to the time-dependent Schrödinger equation. Combining Eq. (9) with its complex conjugate gives

$$\frac{\partial}{\partial t}\rho(\mathbf{r}) = -i\langle\Psi|\left[|\mathbf{r}\rangle\langle\mathbf{r}|,\hat{H}\right]|\Psi\rangle = -i\langle\Psi|\left[\hat{\rho}(\mathbf{r}),\hat{H}\right]|\Psi\rangle, \tag{28}$$

where $\hat{\rho}(\mathbf{r})$ is the particle density operator. We use atomic units throughout with an electron charge of -1.

Consider the simplest case of a Hamiltonian of the form $\hat{H}^{\text{loc}} = \hat{\mathbf{p}}^2/2 + \hat{V}^{\text{loc}}$ where $\hat{\mathbf{p}}$ is the momentum operator and $\hat{V}^{\text{loc}} = \int\hat{\rho}(\mathbf{r})V(\mathbf{r})d^3r$ is a local scalar potential. The local potential commutes with the density operator, so the only contribution to the current is from the momentum operator. Comparing Eqs. (27) and (28) results in a current-density operator of the form[23]

$$\begin{aligned}\hat{\mathcal{J}}^{\text{loc}}_\alpha(\mathbf{r}) &= -\frac{1}{2}\left[|\mathbf{r}\rangle\langle\mathbf{r}|\hat{p}_\alpha + \hat{p}_\alpha|\mathbf{r}\rangle\langle\mathbf{r}|\right]\\ &= -\frac{1}{2}\left\{\hat{\rho}(\mathbf{r}),\hat{p}_\alpha\right\}.\end{aligned} \tag{29}$$

Using Eq. (20), we have

$$\hat{\mathcal{J}}_\alpha^{\mathrm{loc}}(\mathbf{q}) = -\frac{1}{2}\left(e^{-i\mathbf{q}\cdot\hat{\mathbf{r}}}\hat{p}_\alpha + \hat{p}_\alpha e^{-i\mathbf{q}\cdot\hat{\mathbf{r}}}\right), \tag{30}$$

which gives the cell-periodic operator (Appendix A and B)

$$\hat{\mathcal{J}}_\alpha^{\mathbf{k},\mathbf{q},\mathrm{loc}} = -\left(\hat{p}_\alpha^{\mathbf{k}} + \frac{q_\alpha}{2}\right), \tag{31}$$

where $\hat{p}_\alpha^{\mathbf{k}} = -i\hat{\nabla}_\alpha + \hat{k}_\alpha$ is the cell-periodic momentum operator ($\hat{\nabla}_\alpha$ is a spatial derivative in the α direction, and the overall minus sign is from the electron charge).

2. *Continuity condition and nonlocal potentials*

As mentioned above, *nonlocal* potentials are ubiquitous in almost all modern pseudopotential implementations of DFT.[25–28] When nonlocal potentials are present in the Hamiltonian, the current density in Eq. (29) does not satisfy the continuity equation.

To see this, consider a Hamiltonian with a nonlocal potential: $\hat{H}^{\mathrm{nl}} = \hat{\mathbf{p}}^2/2 + \hat{V}^{\mathrm{loc}} + \hat{V}^{\mathrm{nl}}$ with $\hat{V}^{\mathrm{nl}} = \int d^3r \int d^3r' \hat{\rho}(\mathbf{r},\mathbf{r}')V(\mathbf{r},\mathbf{r}')$ where $\hat{\rho}(\mathbf{r},\mathbf{r}') = |\mathbf{r}\rangle\langle\mathbf{r}'|$. In this case there is an additional term in Eq. (28); using the adiabatic expansion from the previous section, this term is

$$\begin{aligned}\rho_\lambda^{\mathrm{nl}}(\mathbf{r}) = -i\Big(&\langle\psi|\left[\hat{\rho}(\mathbf{r}),\hat{V}^{\mathrm{nl}}\right]|\delta\psi\rangle \\ &+ \langle\delta\psi|\left[\hat{\rho}(\mathbf{r}),\hat{V}^{\mathrm{nl}}\right]|\psi\rangle\Big),\end{aligned} \tag{32}$$

where the subscript on $\rho_\lambda^{\mathrm{nl}}(\mathbf{r})$ indicates that it is the induced density from an adiabatic perturbation parameterized by λ. If we write the total induced current as the sum of contributions from the local and nonlocal parts, $\mathbf{J} = \mathbf{J}^{\mathrm{loc}} + \mathbf{J}^{\mathrm{nl}}$, then we have

$$\nabla\cdot\mathbf{J}^{\mathrm{nl}}(\mathbf{r}) = -\rho_\lambda^{\mathrm{nl}}(\mathbf{r}). \tag{33}$$

This "nonlocal charge", $\rho_\lambda^{\mathrm{nl}}$, measures the degree to which the continuity equation, Eq. (27), breaks down if Eq. (29) is used in a nonlocal pseudopotential context.

Li *et al.*[24] argued that such nonlocal charge could be used to reconstruct the nonlocal contribution to the current density via a Poisson equation. Indeed, Eq. (33) indicates that the irrotational part of $\mathbf{J}^{\mathrm{nl}}$ can be determined by calculating Eq. (32). Their approach yields a conserved current by construction, but there are two additional requirements that a physically meaningful definition of the quantum-mechanical electronic current should satisfy:

- The nonlocality of the Hamiltonian should be confined to small spheres surrounding the ionic cores. In the interstitial regions, the nonlocal part of the pseudopotentials vanishes and the Hamiltonian operator is local therein. Thus, the current-density operator should reduce to the simple textbook formula outside the atomic spheres. The corollary is that $\mathbf{J}^{\mathrm{nl}}(\mathbf{r})$ must vanish in the interstitial regions.

- The macroscopic average of the microscopic current should reduce to the well-known expression $\hat{v}_\alpha = -i[\hat{r}_\alpha, \hat{H}]$ for the electronic velocity operator.[45–48] This is routinely used in the context of DFPT, e.g., to calculate the polarization response to ionic displacements needed for the Born effective charge tensor.

The strategy proposed by Li *et al.*[24] falls short of fulfilling either condition. Regarding the first (spatial confinement), note that the nonlocal charge associated to individual spheres generally has a nonzero dipole (and higher multipole) moments. Therefore, even if the nonlocal charge is confined to the sphere, an irrotational field whose divergence results in such a charge density will generally have a long-ranged character and propagate over all space.

Regarding the relation to the macroscopic particle velocity, note that the construction proposed by Li *et al.*[24] in practice discards the solenoidal part of the nonlocal current and hence fails at describing its contribution to the transverse polarization response. This is precisely the quantity we are interested in in the context of flexoelectricity, and is also crucial for obtaining other important quantities, such as the Born charge tensor, that are part of standard DFPT implementations.

Therefore, a calculation of Eqs. (32) does not contain the necessary information to determine $\mathbf{J}^{\mathrm{nl}}$, and an alternative derivation to the textbook one outlined in Sec. III B 1 is required.

3. *Current-density operator generalized for nonlocal potentials*

In light of the previous section, we will now focus on determining an expression for $\hat{\mathcal{J}}_\alpha$ that is applicable when nonlocal potentials are present in the Hamiltonian. For the case of a perturbation that is uniform over the crystal, corresponding to the long wavelength, $\mathbf{q} = 0$ limit of Eq. (3), it is well known that the momentum operator should be replaced with the canonical velocity operator $\hat{v}_\alpha$[45–48] in order to determine the *macroscopic* current.

In Ref. 29, the expression for the *microscopic* current operator that was used to calculate the current induced by a uniform electric field was Eq. (29) with $\hat{p}_\alpha$ replaced by $\hat{v}_\alpha$. Although this treatment will result in the correct current when averaged over a unit cell, this operator does not satisfy the continuity condition in Eq. (27) except in the special case of a Hamiltonian with only local potentials, where it reduces to Eq. (29).

We shall be treating a long wavelength acoustic phonon in this study, and we require the polarization response be correct at least to second order in $\mathbf{q}$ [*cf.* Eq. (7)].

Therefore, we require a version of $\hat{v}_\alpha$ that is designed to handle spatially varying perturbations.

For an arbitrary electronic Hamiltonian $H^{\mathbf{A}}$ coupled to a vector potential $\mathbf{A}(\mathbf{r})$, the most general form for the current-density operator is

$$\hat{\mathcal{J}}_\alpha(\mathbf{r}) = -\frac{\partial \hat{H}^{\mathbf{A}}}{\partial A_\alpha(\mathbf{r})}. \tag{34}$$

Our perturbing vector potential will be a long-wavelength acoustic phonon of wavevector $\mathbf{q}$, and we are interested in the response occurring at the same wavevector $\mathbf{q}$. It is thus useful to define

$$\hat{\mathcal{J}}_\alpha(\mathbf{r}) = \sum_{\mathbf{G}} \hat{\mathcal{J}}_\alpha(\mathbf{G}+\mathbf{q}) e^{i(\mathbf{G}+\mathbf{q})\cdot\mathbf{r}}, \tag{35}$$

$$A_\alpha(\mathbf{r}) = \sum_{\mathbf{G}} A_\alpha(\mathbf{G}+\mathbf{q}) e^{i(\mathbf{G}+\mathbf{q})\cdot\mathbf{r}}, \tag{36}$$

$$P_{\alpha,\kappa\beta\mathbf{q}}(\mathbf{r}) = \sum_{\mathbf{G}} P_{\alpha,\kappa\beta\mathbf{q}}(\mathbf{G}+\mathbf{q}) e^{i(\mathbf{G}+\mathbf{q})\cdot\mathbf{r}}. \tag{37}$$

With these definitions, Eq. (34) becomes

$$\hat{\mathcal{J}}_\alpha(\mathbf{G}+\mathbf{q}) = -\frac{\partial \hat{H}^{\mathbf{A}}}{\partial A^*_\alpha(\mathbf{G}+\mathbf{q})} \tag{38}$$

and the desired operator for Eq. (21) is

$$\hat{\mathcal{J}}_\alpha(\mathbf{q}) = -\frac{\partial \hat{H}^{\mathbf{A}}}{\partial A^*_\alpha(\mathbf{q})}. \tag{39}$$

Again, if the Hamiltonian of interest had the form of $H^{\mathrm{loc}} = (\hat{\mathbf{p}} + \hat{\mathbf{A}})^2/2 + \hat{V}^{\mathrm{loc}}$, where the scalar potential is local and $\hat{\mathbf{A}} = \int \hat{\rho}(\mathbf{r})\mathbf{A}(\mathbf{r})d^3r$ is a local vector potential, then $\hat{\mathcal{J}}^{\mathrm{loc}}_\alpha(\mathbf{r}) = -\frac{1}{2}\left\{\hat{\rho}(\mathbf{r}), (\hat{p}_\alpha + \hat{A}_\alpha)\right\}$. However, for our implementation, we are considering the case where the potential $\hat{V}$ is nonlocal, so we must determine how to couple a generally nonlocal Hamiltonian to a spatially nonuniform vector potential field (which will be the case for a finite $\mathbf{q}$ perturbation).

The standard strategy for describing the coupling to the vector potential is to multiply the nonlocal operator by a complex phase containing the line integral of the vector potential $\mathbf{A}$;[31,35,49] in the real-space representation:

$$\mathcal{O}^{\mathbf{A}}(\mathbf{s},\mathbf{s}') = \mathcal{O}(\mathbf{s},\mathbf{s}') e^{-i\int_{\mathbf{s}'\to\mathbf{s}} \mathbf{A}\cdot d\ell}. \tag{40}$$

The different methods that have been proposed for coupling $\mathbf{A}$ to a nonlocal Hamiltonian amount to applying the complex phase in Eq. (40) to either the entire Hamiltonian[49] or just the nonlocal potential,[31,35] and choosing either a straight-line path[31,49] or a path that passes through the centers of the atoms[35] to perform the line integral.

4. Straight-line path

Using Feynman path integrals, Ismail-Beigi, Chang, and Louie[31] (ICL) derived the following form of a nonlocal Hamiltonian coupled to a vector potential field:

$$\begin{aligned}\hat{H}^{\mathbf{A}}_{\mathrm{ICL}} &= \frac{1}{2}(\hat{\mathbf{p}} + \hat{\mathbf{A}})^2 + \hat{V}^{\mathrm{loc}} \\ &\quad + \int d^3s \int d^3s' \hat{\rho}(\mathbf{s},\mathbf{s}') V^{\mathrm{nl}}(\mathbf{s},\mathbf{s}') e^{-i\int_{\mathbf{s}'}^{\mathbf{s}} \mathbf{A}\cdot d\ell},\end{aligned} \tag{41}$$

where the line integral is taken along a straight path from $\mathbf{s}$ to $\mathbf{s}'$. We will demonstrate that this is equivalent to the approach of Essin *et al.*, where the coupled Hamiltonian is written

$$H^{\mathbf{A}}(\mathbf{s},\mathbf{s}') = H(\mathbf{s},\mathbf{s}') e^{-i\int_{\mathbf{s}'}^{\mathbf{s}} \mathbf{A}\cdot d\ell}, \tag{42}$$

i.e., all of the $\mathbf{A}$ dependence is contained in the complex phase, and the line integral is also taken along a straight path from $\mathbf{s}$ to $\mathbf{s}'$.

Expanding Eq. (42) to first order gives

$$H^{\mathbf{A}}(\mathbf{s},\mathbf{s}') = H(\mathbf{s},\mathbf{s}') - iH(\mathbf{s},\mathbf{s}') \int_{\mathbf{s}'}^{\mathbf{s}} \mathbf{A}\cdot d\ell + \cdots. \tag{43}$$

We would like to evaluate Eq. (39) for this form of the Hamiltonian. Since $\mathbf{A}(\mathbf{r})$ is real we can write Eq. (36) as $A_\alpha(\mathbf{r}) = A^*_\alpha(\mathbf{r}) = A^*_\alpha(\mathbf{q})e^{-i\mathbf{q}\cdot\mathbf{r}}$ so that the integral over $\mathbf{A}$ for the ICL[31] path is

$$\begin{aligned}\int_{\mathbf{s}'}^{\mathbf{s}} \mathbf{A}\cdot d\ell &= \int_0^1 d\tau \mathbf{A}[\mathbf{s}' + \tau(\mathbf{s}-\mathbf{s}')]\cdot(\mathbf{s}-\mathbf{s}') \\ &= \mathbf{A}^*(\mathbf{q})\cdot(\mathbf{s}-\mathbf{s}')\int_0^1 d\tau e^{-i\mathbf{q}\cdot[\mathbf{s}'+\tau(\mathbf{s}-\mathbf{s}')]} \\ &= -\mathbf{A}^*(\mathbf{q})\cdot(\mathbf{s}-\mathbf{s}')\frac{e^{-i\mathbf{q}\cdot\mathbf{s}} - e^{-i\mathbf{q}\cdot\mathbf{s}'}}{i\mathbf{q}\cdot(\mathbf{s}-\mathbf{s}')}\end{aligned} \tag{44}$$

Therefore, from Eqs. (43) and (39),

$$\langle \mathbf{s}|\hat{\mathcal{J}}^{\mathrm{ICL}}_\alpha(\mathbf{q})|\mathbf{s}'\rangle = -iH(\mathbf{s},\mathbf{s}')(s_\alpha - s'_\alpha)\frac{e^{-i\mathbf{q}\cdot\mathbf{s}} - e^{-i\mathbf{q}\cdot\mathbf{s}'}}{i\mathbf{q}\cdot(\mathbf{s}-\mathbf{s}')}. \tag{45}$$

In practice we shall normally work in terms of the cell-periodic current operator of Eq. (23), whose position representation follows as

$$\langle \mathbf{s}|\hat{\mathcal{J}}^{\mathbf{k},\mathbf{q},\mathrm{ICL}}_\alpha|\mathbf{s}'\rangle = -iH^{\mathbf{k}}(\mathbf{s},\mathbf{s}')(s_\alpha - s'_\alpha)\frac{e^{-i\mathbf{q}\cdot(\mathbf{s}-\mathbf{s}')} - 1}{i\mathbf{q}\cdot(\mathbf{s}-\mathbf{s}')}. \tag{46}$$

We can see that the current operator of Eq. (45) satisfies the continuity condition of Eq. (27) as follows. In reciprocal space the continuity equation becomes $i\mathbf{q}\cdot[-\hat{\mathcal{J}}^{\mathrm{ICL}}(\mathbf{q})] = -\partial\hat{\rho}_{\mathbf{q}}/\partial t$, where $\hat{\rho}_{\mathbf{q}} = e^{-i\mathbf{q}\cdot\hat{\mathbf{r}}}$ is the $\mathbf{G}=0$ particle density operator for a given $\mathbf{q}$, and the negative sign in front of the current operator reflects the sign of the electron charge. But from Eq. (45) it quickly follows that

$$-i\mathbf{q}\cdot\langle \mathbf{s}|\hat{\mathcal{J}}^{\mathrm{ICL}}_\alpha(\mathbf{q})|\mathbf{s}'\rangle = i\langle \mathbf{s}|\left[\hat{\rho}_{\mathbf{q}}, \hat{H}\right]|\mathbf{s}'\rangle \tag{47}$$

which, using the Ehrenfest theorem, is nothing other than $-\partial\hat{\rho}_{\mathbf{q}}/\partial t$ in the position representation.

In the case that only local potentials are present, only the kinetic term in the Hamiltonian contributes to $\hat{\mathcal{J}}_\alpha^{\mathrm{ICL}}(\mathbf{q})$. We show in Appendix A that the current operator then reduces to the form of Eq. (30). The fact that the local and nonlocal parts can be separated demonstrates the equivalence of the ICL [Eq. (41)] and Essin *et al.* [Eq. (42)] approaches.

In the case that nonlocal potentials are present, we show in Appendix A that, for $\mathbf{q} = 0$, Eq. (45) reduces to the well-known expression for the canonical velocity operator[45–48] $\hat{\mathcal{J}}_\alpha^{\mathrm{ICL}}(\mathbf{q}=0) = -\hat{v}_\alpha = i\left[\hat{r}_\alpha, \hat{H}\right]$, where the -1 comes from the electron charge. We discuss the case of nonlocal potentials and finite $\mathbf{q}$ perturbations in Sec. III C.

5. Path through atom center

Subsequently, Pickard and Mauri[32] (PM) proposed using a path from $\mathbf{s}$ to the atom center, $\mathbf{R}$, and then to $\mathbf{s}'$, which was constructed explicitly to give better agreement for magnetic susceptibility between pseudopotential and all-electron calculations. Their approach was to use a coupled Hamiltonian of the form

$$\hat{H}_{\mathrm{PM}}^{\mathbf{A}} = \frac{1}{2}(\hat{\mathbf{p}} + \hat{\mathbf{A}})^2 + \hat{V}^{\mathrm{loc}} + \sum_{\zeta=1}^{N} \int d^3s \int d^3s' \times \hat{\rho}(\mathbf{s},\mathbf{s}') V_\zeta^{\mathrm{nl}}(\mathbf{s},\mathbf{s}') e^{-i\int_{\mathbf{s}'\to\mathbf{R}_\zeta\to\mathbf{s}} \mathbf{A}\cdot d\ell}, \tag{48}$$

where N is the number of atoms in the cell, $\mathbf{R}_\zeta$ is the position of atom ζ, and V_ζ^{nl} is the nonlocal potential for that atom. The PM approach explicitly splits the nonlocal contribution from $\mathbf{A}$ into contributions from each atomic sphere centered at $\mathbf{R}_\zeta$.[50] Therefore, the total current operator is

$$\hat{\mathcal{J}}_\alpha^{\mathbf{k},\mathbf{q},\mathrm{PM}} = -\left(\hat{p}_\alpha^{\mathbf{k}} + \frac{q_\alpha}{2}\right) + \sum_{\zeta=1}^{N} \hat{\mathcal{J}}_{\alpha,\zeta}^{\mathbf{k},\mathbf{q},\mathrm{PM,nl}}, \tag{49}$$

where the superscript "nl" and the subscript ζ emphasize that each item in the summation describes the contribution to the current from the nonlocal potential of the atom ζ; it is obvious from Eqs. (48) and (49) that $\hat{\mathcal{J}}_\alpha^{\mathrm{loc}}$ will be recovered in the case of a local potential.

For an atom at position $\mathbf{R}_\zeta$, the line integral in Eq. (48) is

$$\int_{\mathbf{s}'\to\mathbf{R}_\zeta\to\mathbf{s}} \mathbf{A}\cdot d\ell = -\mathbf{A}^*(\mathbf{q})\cdot(\mathbf{R}_\zeta - \mathbf{s}')\frac{e^{-i\mathbf{q}\cdot\mathbf{R}_\zeta} - e^{-i\mathbf{q}\cdot\mathbf{s}'}}{i\mathbf{q}\cdot(\mathbf{R}_\zeta - \mathbf{s}')} - \mathbf{A}^*(\mathbf{q})\cdot(\mathbf{s} - \mathbf{R}_\zeta)\frac{e^{-i\mathbf{q}\cdot\mathbf{s}} - e^{-i\mathbf{q}\cdot\mathbf{R}_\zeta}}{i\mathbf{q}\cdot(\mathbf{s} - \mathbf{R}_\zeta)}. \tag{50}$$

Therefore we have

$$\langle \mathbf{s}|\hat{\mathcal{J}}_{\alpha,\zeta}^{\mathrm{PM,nl}}(\mathbf{q})|\mathbf{s}'\rangle = -iV_\zeta^{\mathrm{nl}}(\mathbf{s},\mathbf{s}')\left[(R_{\alpha,\zeta} - s'_\alpha)\frac{e^{-i\mathbf{q}\cdot\mathbf{R}_\zeta} - e^{-i\mathbf{q}\cdot\mathbf{s}'}}{i\mathbf{q}\cdot(\mathbf{R}_\zeta - \mathbf{s}')} + (s_\alpha - R_{\alpha,\zeta})\frac{e^{-i\mathbf{q}\cdot\mathbf{s}} - e^{-i\mathbf{q}\cdot\mathbf{R}_\zeta}}{i\mathbf{q}\cdot(\mathbf{s} - \mathbf{R}_\zeta)}\right], \tag{51}$$

so the cell-periodic operator is

$$\langle \mathbf{s}|\hat{\mathcal{J}}_{\alpha,\zeta}^{\mathbf{k},\mathbf{q},\mathrm{PM,nl}}|\mathbf{s}'\rangle = -iV_\zeta^{\mathrm{nl}}(\mathbf{s},\mathbf{s}')\left[(R_{\alpha,\zeta} - s'_\alpha)\frac{e^{-i\mathbf{q}\cdot(\mathbf{R}_\zeta - \mathbf{s}')} - 1}{i\mathbf{q}\cdot(\mathbf{R}_\zeta - \mathbf{s}')} + (s_\alpha - R_{\alpha,\zeta})\frac{e^{-i\mathbf{q}\cdot(\mathbf{s} - \mathbf{s}')} - e^{-i\mathbf{q}\cdot(\mathbf{R}_\zeta - \mathbf{s}')}}{i\mathbf{q}\cdot(\mathbf{s} - \mathbf{R}_\zeta)}\right]. \tag{52}$$

From Eqs. (51) and (32), we see that $i\mathbf{q}\cdot[-\hat{\mathcal{J}}^{\mathrm{PM,nl}}(\mathbf{q})] = i\left[e^{-i\mathbf{q}\cdot\hat{\mathbf{r}}}, \hat{V^{\mathrm{nl}}}\right] = -\hat{\rho}_\lambda^{\mathrm{nl}}$. Therefore, Eq. (49) satisfies the continuity condition. Also, in the case of a $\mathbf{q} = 0$ perturbation, $\hat{\mathcal{J}}_\alpha^{\mathrm{PM,nl}}(\mathbf{q}=0) = i\left[\hat{r}_\alpha, \hat{V}^{\mathrm{nl}}\right]$, which is the nonlocal contribution to $-\hat{v}_\alpha$, as expected. We discuss the case of nonlocal potentials and finite $\mathbf{q}$ perturbations in the next section.

Finally, we see that for the longitudinal response (where $\mathbf{q} = q_\alpha\hat{\alpha}$), the ICL and PM approaches produce identical operators. This is expected, since they both satisfy the continuity equation. Only circulating currents (e.g., transverse or shear FxE components) may exhibit path dependence.

C. Long wavelength expansion

Recall that only the induced polarization up to second order in $\mathbf{q}$ is required for the FxE coefficients [*cf.* Eq. (7)]. Therefore, instead of attempting to calculate Eq. (26) with either Eq. (46) or (49) directly, we will expand these expressions for the current-density operator to second order in $\mathbf{q}$.

Considering the Hamiltonian in Eq. (14), there are contributions to $\hat{\mathcal{J}}_\alpha^{\mathbf{q}}$ from the kinetic energy and nonlocal part of the pseudopotential. We show in Appendix A [Eq. (A4)] that the kinetic energy only contributes up to first order in $\mathbf{q}$, and for a local Hamiltonian, the current operator reduces to the form of Eq. (31).

The nonlocal potential will, however, contribute at all orders. As mentioned in Sec. III B 4 and III B 5, for $\mathbf{q}=0$, both the ICL and PM approaches give $\hat{\mathcal{J}}_\alpha^{\mathbf{k},\mathbf{q}=0} = -\hat{v}_\alpha^{\mathbf{k}} = i[\hat{r}_\alpha, \hat{H}^{\mathbf{k}}] = -\hat{p}_\alpha^{\mathbf{k}} + \hat{\mathcal{J}}_\alpha^{\mathbf{k},\mathrm{nl}(0)}$, where we have defined $\hat{\mathcal{J}}_\alpha^{\mathbf{k},\mathrm{nl}(0)} \equiv i[\hat{r}_\alpha, \hat{V}^{\mathbf{k},\mathrm{nl}}]$. At higher orders in $\mathbf{q}$, and for nonlongitudinal response, the ICL and PM approaches may no longer agree.

Up to second order in $\mathbf{q}$, the current operator can be written as

$$\begin{aligned}\hat{\mathcal{J}}_\alpha^{\mathbf{k},\mathbf{q}} \simeq &-\left(\hat{p}_\alpha^{\mathbf{k}} + \frac{q_\alpha}{2}\right) + \hat{\mathcal{J}}_\alpha^{\mathbf{k},\mathrm{nl}(0)} \\ &+ \frac{q_\gamma}{2}\hat{\mathcal{J}}_{\alpha,\gamma}^{\mathbf{k},\mathrm{nl}(1)} + \frac{q_\gamma q_\xi}{6}\hat{\mathcal{J}}_{\alpha,\gamma\xi}^{\mathbf{k},\mathrm{nl}(2)},\end{aligned} \tag{53}$$

where the higher order terms in $\mathbf{q}$, $\hat{\mathcal{J}}_{\alpha,\gamma}^{\mathbf{k},\mathbf{q},\mathrm{nl}(1)}$ and $\hat{\mathcal{J}}_{\alpha,\gamma\xi}^{\mathbf{k},\mathbf{q},\mathrm{nl}(2)}$, are the result of the nonlocal part of the Hamiltonian *and* the fact that the monochromatic perturbation is nonuniform (finite $\mathbf{q}$). Plugging the current operator from Eq. (53) into Eq. (26), readily yields the induced polarization,

$$\overline{P}_{\alpha,\kappa\beta}^{\mathbf{q}} = \overline{P}_{\alpha,\kappa\beta}^{\mathbf{q},\mathrm{loc}} + \overline{P}_{\alpha,\kappa\beta}^{\mathbf{q},\mathrm{nl}}, \tag{54}$$

where we have separated the contribution of the local current operator (loc) from the nonlocal (nl) part. The exact expression for $\overline{P}_{\alpha,\kappa\beta}^{\mathbf{q},\mathrm{loc}}$ is derived in Appendix B, yielding Eq. (B8); the approximate (exact only up to second order in $\mathbf{q}$) expression for $\overline{P}_{\alpha,\kappa\beta}^{\mathbf{q},\mathrm{nl}}$ is derived in Appendix C, specifically in Eqs. (C7)-(C10) for the ICL path and Eqs. (C12)-(C14) for the PM path.

D. Dynamic contribution and diamagnetic susceptibility

Transverse or shear strain gradients result in rigid rotations of unit cells which must be treated carefully in order to calculate physically meaningful values of the flexoelectric tensor. This issue can be loosely compared to the well-known distinction between the proper and improper piezoelectric tensor,[51,52] but, in the case of strain gradients, it is complicated by the fact that different parts of the sample typically rotate at different rates. The reader is referred to Ref. 20 for a complete discussion; only the results of that work necessary for our purposes will be reproduced here.

Local rotations of the sample dynamically produce local circulating currents, akin to the diamagnetic currents that are induced by an applied magnetic field. The gradient of a magnetization is a macroscopic current, which implies that this effect implicitly contributes to the flexoelectric coefficients as defined in Eq. (7). As was shown in Ref. 20 (see also Appendix D for an abridged derivation), this "dynamic contribution" only concerns the nonlongitudinal components and is proportional to the diamagnetic susceptibility of the material, $\chi_{\gamma\lambda} = \partial M_\gamma / \partial H_\lambda$ where M is the magnetization and H the magnetic field. Specifically,

$$\overline{P}_{\alpha,\beta}^{(2,\omega\nu),\mathrm{dyn}} = \sum_{\gamma\lambda}\left(\epsilon^{\alpha\omega\gamma}\epsilon^{\beta\lambda\nu} + \epsilon^{\alpha\nu\gamma}\epsilon^{\beta\lambda\omega}\right)\chi_{\gamma\lambda}, \tag{55}$$

where ϵ's are Levi-Civita symbols. It was futher shown in Ref. 20 that the dynamic contribution will not produce an electrically measurable response in an experimental sample, as the *bulk* contribution will exactly cancel with an equal and opposite *surface* contribution. The bulk FxE constants calculated using the formalism in this work will contain both the dynamic and static contributions. In order to report more physically meaningful bulk FxE coefficients that can be directly compared to charge-density-based calculations,[18] we would like to remove the dynamic contribution from our calculated $\overline{P}_{\alpha,\kappa\beta}^{(2,\omega\nu)}$.

To calculate $\chi_{\gamma\lambda}$, there is again a subtlety involved in the use of nonlocal pseudopotentials. Conventional calculations of the diamagnetic susceptibility involve applying a vector potential perturbation and calculating the current response.[30–33,35] In the case of a local Hamiltonian the aforementioned rotational field is indistinguishable from an electromagnetic vector potential, and the expression for $\chi_{\gamma\lambda}$ is identical to the diamagnetic susceptibility. However, in the case of a nonlocal Hamiltonian this is no longer true. In that case, the perturbation remains the *local* current operator, $\hat{\mathcal{J}}^{\mathrm{loc}}$, while the current response is evaluated using the total (local plus nonlocal) $\hat{\mathcal{J}}$ (*cf.* Appendix D). This difference indicates that Larmor's theorem, which states that the effects of a uniform rotation and those of a uniform magnetic field are the same to first order in the field/angular velocity, may break down for nonlocal potentials. This is discussed further in Sec. VI.

IV. IMPLEMENTATION

The procedure for calculating the FxE coefficients using the formalism in Sec. III is as follows. We first perform conventional DFPT phonon calculations [displacing sublattice κ in direction β, as in Eq. (3)] at small but finite wavevectors $\mathbf{q}$ to obtain the static first-order wavefunctions $|\partial_\lambda u_{n\mathbf{k},\mathbf{q}}^{\kappa\beta}\rangle$. We choose $|q| < 0.04$, where here and henceforth we express q in reduced units of $2\pi/a$ (a is the cubic lattice constant). To avoid the sum over empty states in Eq. (11), we determine the first-order adiabatic wavefunctions by solving the Sternheimer equation

$$(H_{\mathbf{k}} - \epsilon_{n\mathbf{k}})|\delta u_{n\mathbf{k},\mathbf{q}}^{\kappa\beta}\rangle = -i\mathcal{Q}_{c,\mathbf{k}+\mathbf{q}}|\partial_\lambda u_{n\mathbf{k},\mathbf{q}}^{\kappa\beta}\rangle \tag{56}$$

where $\epsilon_{n\mathbf{k}}$ is the eigenvalue of band n and k-point $\mathbf{k}$ and $\mathcal{Q}_{c,\mathbf{k}+\mathbf{q}}$ is the projector over conduction band states (implemented as one minus the projector over valence states). Then we apply the current operator in Eq. (53) to obtain $\overline{P}_{\alpha,\kappa\beta}^{\mathbf{q}}$ from Eq. (26) (see Appendix B and C for details).

As will be discussed in Sec. V A, we will use the ICL path for most of the calculations in this study, so the explicit expression for this case is provided in this section. The local contribution to $\overline{P}^{\mathbf{q}}_{\alpha,\kappa\beta}$ is derived in Appendix B, leading to Eq. (B8). The three terms in the small-$\mathbf{q}$ expansion of the nonlocal part are determined in Appendix C 1 by combining Eqs. (46) and (26), and expanding in powers of $\mathbf{q}$, leading to Eq. (C7). Combining Eq. (B8) and (C7) we have

$$\begin{aligned}\overline{P}^{\mathbf{q},\mathrm{ICL}}_{\alpha,\kappa\beta} = -\frac{4}{N_k}\sum_{n\mathbf{k}}\Bigg[&\langle u_{n\mathbf{k}}|\hat{p}^{\mathbf{k}}_{\alpha}+\frac{q_\alpha}{2}|\delta u^{\kappa\beta}_{n\mathbf{k},\mathbf{q}}\rangle + \langle u_{n\mathbf{k}}|\frac{\partial \hat{V}^{\mathbf{k},\mathrm{nl}}}{\partial k_\alpha}|\delta u^{\kappa\beta}_{n\mathbf{k},\mathbf{q}}\rangle \\ &+\frac{1}{2}\sum_{\gamma=1}^{3} q_\gamma \langle u_{n\mathbf{k}}|\frac{\partial^2 \hat{V}^{\mathbf{k},\mathrm{nl}}}{\partial k_\alpha \partial k_\gamma}|\delta u^{\kappa\beta}_{n\mathbf{k},\mathbf{q}}\rangle + \frac{1}{6}\sum_{\gamma=1}^{3}\sum_{\xi=1}^{3} q_\gamma q_\xi \langle u_{n\mathbf{k}}|\frac{\partial^3 \hat{V}^{\mathbf{k},\mathrm{nl}}}{\partial k_\alpha \partial k_\gamma \partial k_\xi}|\delta u^{\kappa\beta}_{n\mathbf{k},\mathbf{q}}\rangle\Bigg],\end{aligned} \tag{57}$$

where we have again assumed TRS [*cf.* Eq. 26]. A similar equation is derived in Appendix C 2 for the PM path.

In order to obtain $\overline{P}^{(2,\omega\nu)}_{\alpha,\kappa\beta}$, we calculate numerical second derivatives with respect to q_ω and q_ν yielding the needed flexoelectric coefficients $\mu^{\mathrm{I}}_{\alpha\beta,\omega\nu}$ via Eq. (7). Note that, in addition to the explicit factors of q multiplying the last two terms, each term has an implicit q dependence through $\delta u^{\kappa\beta}_{n\mathbf{k},\mathbf{q}}$ so all terms may contribute to the second derivative.

Since we will consider cubic materials there are three independent FxE coefficients:[15,17]

$$\begin{aligned}\mu_{\mathrm{L}} &= \mu^{\mathrm{II}}_{11,11} = \mu^{\mathrm{I}}_{11,11},\\ \mu_{\mathrm{S}} &= \mu^{\mathrm{II}}_{12,12} = \mu^{\mathrm{I}}_{11,22},\\ \mu_{\mathrm{T}} &= \mu^{\mathrm{II}}_{11,22} = 2\mu^{\mathrm{I}}_{12,12} - \mu^{\mathrm{I}}_{11,22},\end{aligned} \tag{58}$$

where L stands for longitudinal, S for shear, and T for transverse.

A. Electrostatic boundary conditions

The current response to a phonon perturbation, just like other response properties, displays a strongly nonanalytic behavior in a vicinity of the Γ point ($\mathbf{q}=0$), so some care must be taken when taking the long-wave expansions described in the previous Sections. A long-wave phonon naturally imposes "mixed" electrical (ME) boundary conditions:[17] Along the longitudinal direction ($\hat{\mathbf{q}}$) the electric displacement field, $\mathbf{D}$, must vanish ($\mathbf{D}\cdot\hat{\mathbf{q}}=0$); conversely, periodicity is preserved in the planes that are normal to $\hat{\mathbf{q}}$, resulting in a vanishing electric field therein. In general, the bulk FxE tensor needs to be defined under isotropic "short-circuit" (SC) boundary conditions, which implies that the problematic longitudinal $\mathbf{E}$-fields must be suppressed. In our calculations, this goal can be achieved using the procedure of Refs. 15 and 18, where the $\mathbf{G}=0$ component of the self-consistent first-order potential is removed in the DFPT calculation of $\partial_\lambda u^{\kappa\beta}_{n\mathbf{k},\mathbf{q}}$ [Eq. (56)]. We will use this procedure for the calculations of cubic oxides in Sec. V B.

For several reasons, one may sometimes be interested in calculating the flexoelectric coefficients under mixed electrical boundary conditions; in such a case, of course, the $\mathbf{G}=0$ component of the self-consistent first-order potential should not be removed. Then, however, one must keep in mind that the long-wave expansion of the polarization response is only allowed along a fixed direction in reciprocal space. (This implies performing the calculations at points $\mathbf{q}=q\hat{\mathbf{q}}$, and subsequently operating the Taylor expansion as a function of the one-dimensional parameter q.) In crystals where the macroscopic dielectric tensor is isotropic and $\hat{\mathbf{q}}$ corresponds to a high-symmetry direction, the longitudinal coefficients in and mixed electrical boundary conditions are simply related to the short circuit ones by the dielectric constant, ϵ,

$$\mu^{\mathrm{SC}}_{\mathrm{L}} = \epsilon \mu^{\mathrm{ME}}_{\mathrm{L}}. \tag{59}$$

We will use mixed electrical boundary conditions for our benchmark calculations of noble gas atoms in Sec. V A since, in this particular system, $\mu^{\mathrm{ME}}_{\mathrm{L}}$, rather than $\mu^{\mathrm{SC}}_{\mathrm{L}}$, can be directly compared to the moments of the real-space charge density,[17] as discussed in Sec. V A 1.

B. Magnetic susceptibility contribution

In Sec. III D, we explained that the diamagnetic susceptibility is required in order to correct for the dynamic contribution to the FxE coefficients. To avoid the sum over states in Eq. (D3), we solve the Sternheimer equation

$$(\hat{H}_{\mathbf{k}} - \epsilon_{n\mathbf{k}})|\partial_{\dot{\alpha}} u^{\alpha}_{n\mathbf{k},\mathbf{q}}\rangle = \mathcal{Q}_{c,\mathbf{k}+\mathbf{q}}\left(\hat{p}^{\mathbf{k}}_{\alpha}+\frac{q_\alpha}{2}\right)|u_{n\mathbf{k}}\rangle. \tag{60}$$

Recall that $-\left(\hat{p}^{\mathbf{k}}_{\alpha}+\hat{q}_\alpha/2\right)$ is the cell-averaged current operator in the case of a local potential. We then apply the *full* current operator [Eq. (53)] to obtain Eq. (D4) at several small but finite q (as above, $|q|<0.04$) in order to perform a numerical second derivative and obtain $\overline{P}^{(2,\omega\nu),\ \mathrm{dyn}}_{\alpha,\beta}$ from Eq. (55).

For the case of a material with cubic symmetry, where $\chi_{\alpha\beta} = \chi_{\mathrm{mag}}\delta_{\alpha\beta}$, we see from Eq. (55) that there will

TABLE I. $Q^{\rm RCC}$ for the various atoms in the materials in Sec. V B in units of e Bohr^2.

	$Q^{\rm RCC}$		$Q^{\rm RCC}$
Sr	−5.93	Ba	−13.39
Ti	−0.54	Zr	−4.55
O	−0.01	Pb	−15.16
Mg	−4.85		

be two nonzero elements of the dynamic contribution: $\overline{P}^{(2,22),\,\rm dyn}_{1,1} = 2\chi_{\rm mag}$ and $\overline{P}^{(2,12),\,\rm dyn}_{1,2} = -\chi_{\rm mag}$. Therefore, the clamped-ion FxE constants with the dynamic contribution removed, μ', are given by[20]

$$\begin{aligned} \mu'_{\rm L} &= \mu_{\rm L}, \\ \mu'_{\rm S} &= \mu_{\rm S} - \chi_{\rm mag}, \\ \mu'_{\rm T} &= \mu_{\rm T} + 2\chi_{\rm mag}, \end{aligned} \tag{61}$$

for cubic materials.

C. Rigid-core correction

It was demonstrated in Ref. 16 that the clamped-ion FxE constants depend on the treatment of the core density, which will be different for a different choice of pseudopotential. This dependence is exactly canceled when the surface contribution is calculated consistently with the same pseudopotentials.[53,54] In order to report more "portable" values for the bulk FxE coefficients, we apply the rigid-core correction (RCC) of Refs. 16 and 17:

$$Q^{\rm RCC}_\kappa = 4\pi \int dr r^4 \left[\rho^{\rm AE}_\kappa(\mathbf{r}) - \rho^{\rm PS}_\kappa(\mathbf{r})\right], \tag{62}$$

where $\rho^{\rm AE}_\kappa(r)$ is the all-electron density of the free atom of type κ, and $\rho^{\rm PS}_\kappa(r)$ is the corresponding pseudocharge density. In Table I we list $Q^{\rm RCC}$ for the various atoms that we will require for the cubic oxides reported below (no RCC is included for the noble gas atoms in Sec. V A). Specifically, for short circuit boundary conditions, $\epsilon \sum_\kappa Q^{\rm RCC}_\kappa/6\Omega$ must be added to $\mu_{\rm L}$ and $\mu_{\rm T}$.[54]

D. Computational details

We have implemented the procedure for calculating the FxE coefficients in the ABINIT code.[55] The PBE generalized gradient approximation functional[56] is used throughout. The conventional phonon and dielectric constant calculations are carried out using the DFPT implementation available in the code.[57,58] In order to solve the nonselfconsistent Sternheimer Eqs. (60) and (56), ABINIT's implementation of the variational approach of Ref. 42 is used.

The nuclei and core electrons are described with optimized norm-conserving Vanderbilt pseudopotentials[59] provided by ABINIT. For the cubic oxides, a $8 \times 8 \times 8$ Monkhorst-Pack[60] k-point mesh is used to sample the Brillouin zone, and the plane-wave energy cutoff is set of 60 Ha. For the isolated atoms, a $2 \times 2 \times 2$ k-point mesh is used, and the plane-wave energy cutoff is set of 70 Ha.

V. RESULTS

A. Benchmark test: Isolated noble gas atoms

1. *Isolated rigid charge model*

In order to test the implementation described in Sec. IV, we consider the toy model of a material made of rigid noninteracting spherical charge distributions arranged in a simple cubic lattice, as explored in Refs. 20, 53, and 54. We shall refer to this henceforth as the "isolated rigid charge" (IRC) model. Of course, such a material is fictitious, since it would have no interatomic forces to hold it together; even so, it serves as an interesting test case since its FxE properties can be determined analytically and compared to our numerical calculations. In this section, we will briefly summarize the expectations of the IRC model (see Refs. 20 and 53 for a more complete discussion).

For the IRC "material," there is only one sublattice per cell. Each "atom" is represented by a spherically symmetric charge density $\rho_{\rm IRC}(r)$ that falls to zero beyond a cutoff r_c chosen small enough to insure that the atomic spheres do not overlap. The atoms are assumed to be neutral, $\int_0^{r_c} \rho_{\rm IRC}(r)\, r^2\, dr = 0$. It was shown in Ref. 20 that the longitudinal and shear coefficients for the IRC model calculated from the current-density implementation are

$$\mu_{\rm L,IRC} = \mu_{\rm S,IRC} = \frac{Q_{\rm IRC}}{2\Omega}, \tag{63}$$

where $\Omega = a^3$ is the cell volume, and

$$Q_{\rm IRC} = \int d^3r \rho_{\rm IRC}(r) x^2 \tag{64}$$

is the quadrupolar moment of the atomic charge density (of course the direction x is arbitrary since the charge density is spherically symmetric).

The FxE constants in Eq. (63) include the dynamic contribution to the current discussed in Sec. III D.[18,20,54] Removing this contribution from our bulk coefficients [see Eq. (61)] results in the primed coefficients for the IRC model[20]

$$\mu'_{\rm L,IRC} = \frac{Q_{\rm IRC}}{2\Omega}, \quad \mu'_{\rm S,IRC} = 0, \tag{65}$$

where the dynamic contribution is given by

$$\chi_{\rm mag,IRC} = \mu_{\rm S,IRC} = \frac{Q_{\rm IRC}}{2\Omega} \tag{66}$$

If we assume that Larmor's theorem holds (i.e., that the dynamic contribution is identical to the magnetic susceptibility), Eq. (66) is just a statement of the Langevin theory of diamagnetism, which relates the magnetic susceptibility to the quadrupole moment of a spherical atomic charge (see Sec. VI).

2. Noble gas atoms

In the following subsections (V A 3, V A 4, V A 5), we will compare the behavior of this model with the results of DFT calculations on isolated noble gas atoms. Several points should be considered when comparing the results of such calculations to the expectations of the IRC model (relations in Sec. V A 1).

Firstly, the noble gas atoms in our DFT calculations are slightly polarizable, i.e., not perfectly described by rigid charge densities. For this reason the longitudinal FxE coefficient will depend on the choice of electrostatic boundary conditions (see Sec. IV A). We will use mixed electrical boundary conditions, where we should find [analogously to Eq. (63)]

$$\mu_{\mathrm{L,NG}}^{\mathrm{ME}} = \frac{Q_{\mathrm{NG}}}{2\Omega}, \tag{67}$$

where the subscript "NG" indicates the DFT calculation on a noble gas atom, and Q_{NG} is the quadropole moment of the unperturbed, ground-state charge density of the noble gas atom. If we had used short circuit boundary conditions, there would have been a factor of ϵ on the right-hand side of Eq. (67). Of course, in the IRC model, the "atoms" are neutral, rigid, and spherical, so $\epsilon = 1$, and, from Eq. (59), short circuit and mixed electric boundary conditions give the same FxE coefficients.

Also, since our noble-gas-atom calculations will use nonlocal pseudopotentials, the equality of $\mu_{\mathrm{S,NG}}$ and $Q_{\mathrm{NG}}/2\Omega$ is not guaranteed; in fact, we will see in Sec. V A 5 that they are not equal, indicating that translational invariance is broken for our current-density formulation in the presence of nonlocal pseudopotentials. Similarly, we will find that χ_{mag} does not equal $Q_{\mathrm{NG}}/2\Omega$ [*cf.* Eq. (66)], indicating that Larmor's theorem also breaks down for our form of the current in the presence of nonlocal pseudopotentials. These issues will be discussed in Sec. VI.

Note that, as with the IRC model, we will drop the κ subscript when discussing the noble gas atoms since the "crystals" that we are considering have only a single sublattice. Also, as all calculations will use mixed electrical boundary condition, we will drop the explicit "ME" labels.

3. Computational strategy: Real-space moments of the charge density

In addition to the relations in Eqs. (63), (65), and (66) of Sec. V A 1 and Eq. (67) of Sec. V A 2, we can perform specific tests of the components of our implementation by exploiting the correspondence between two methods of calculating the FxE coefficients: (i) The long-wavelength expansion in reciprocal space of the polarization induced by a phonon [i.e., Eq. (7)] that we have described so far in this work, and (ii) the computation of the real-space moments of the induced microscopic polarization or charge density from the displacement of an isolated atom in a crystal.[15,17] For the case of the isolated noble gas atoms, displacing the entire sublattice (i.e., applying a $\mathbf{q}$=0 acoustic phonon perturbation) is equivalent to displacing a single atom.

It is particularly useful to compare our methodology to the real-space moments of the induced charge density, since they can be readily calculated from a conventional, DFPT phonon calculation (with $\mathbf{q} = 0$). Specifically, the longitudinal noble-gas response in direction α is[15,17]

$$\mu_{\mathrm{L,NG}} = -\frac{1}{2}\frac{\partial^2 \overline{P}^{\mathbf{q},\mathrm{NG}}_{\alpha,\alpha}}{\partial q_\alpha^2}\bigg|_{\mathbf{q}=0} = \frac{1}{6\Omega}\int_{\mathrm{cell}} d^3r \rho^{\mathrm{NG}}_{\alpha\mathbf{q}=0}(\mathbf{r}) r_\alpha^3. \tag{68}$$

where $\rho^{\mathrm{NG}}_{\alpha\mathbf{q}}(\mathbf{r}) \equiv \partial\rho^{\mathrm{NG}}(\mathbf{r})/\partial\lambda_{\alpha\mathbf{q}}$ is the first-order induced charge density from a phonon with wavevector $\mathbf{q}$ and noble gas atoms displaced in the α direction. $\overline{P}^{\mathbf{q}}_{\alpha,\alpha}$ is calculated with mixed electrical boundary conditions. As mentioned in Sec. V A 2, the right-hand side of Eq. (68) equals $Q_{\mathrm{NG}}/2\Omega$. Recall that, since the charge density is related to the divergence of the polarization, it only gives the longitudinal FxE coefficient. Therefore, we can only use an expression like the one on Eq. (68) to test our implementation of μ_{L}.

In general (i.e., not specific to the case of the isolated noble gas atoms), the induced charge density can be split into contributions from the local and nonlocal parts of the Hamiltonian, as we did for the polarization in Eq. (54). Using the continuity condition, we can write the first-order charge as

$$\rho_{\alpha\mathbf{q}}(\mathbf{G}+\mathbf{q}) = -i(\mathbf{G}+\mathbf{q})\cdot\mathbf{P}^{\mathrm{loc}}_{\alpha\mathbf{q}}(\mathbf{G}+\mathbf{q}) + \rho^{\mathrm{nl}}_{\alpha\mathbf{q}}(\mathbf{G}+\mathbf{q}). \tag{69}$$

Here $\mathbf{P}^{\mathrm{loc}}_{\alpha\mathbf{q}}$ is the "local" part of the induced polarization and $\rho^{\mathrm{nl}}_{\alpha\mathbf{q}}$ is the nonlocal charge introduced in Sec. III B 2. Using the reciprocal-space version of Eq. (29), the local induced polarization is (assuming TRS)

$$P^{\mathrm{loc}}_{\alpha,\alpha\mathbf{q}}(\mathbf{G}+\mathbf{q}) = -\frac{2}{N_k}\sum_{n\mathbf{k}}\langle\psi_{n\mathbf{k}}|\left\{e^{-i(\mathbf{G}+\mathbf{q})\cdot\hat{\mathbf{r}}}, \hat{p}_\alpha\right\}|\delta\psi^\alpha_{n\mathbf{k},\mathbf{q}}\rangle \tag{70}$$

and the nonlocal charge density from Eq. (32) is given

(in reciprocal space) by

$$\rho^{\rm nl}_{\alpha\mathbf{q}}(\mathbf{G}+\mathbf{q}) = -\frac{4i}{N_k}\sum_{n\mathbf{k}}\langle\psi_{n\mathbf{k}}|\left[e^{-i(\mathbf{G}+\mathbf{q})\cdot\hat{\mathbf{r}}},\hat{V}^{\rm nl}\right]|\delta\psi^{\alpha}_{n\mathbf{k},\mathbf{q}}\rangle \tag{71}$$

The first-order charge on the left-hand side of Eq. (69) can be obtained from a conventional DFPT phonon calculation, and thus Eq. (69) allows for several tests of our methodology.

A simple test of the nonlocal contribution at $\mathbf{q}=0$ is to compare the dipole moment of the nonlocal charge with $\overline{P}^{\mathbf{q},\mathrm{nl}(0)}_{\alpha,\alpha}$ [i.e., the second term in Eq. (57)], which should give the nonlocal contribution to the Born effective charge

$$Z^{*}_{\alpha\beta,\mathrm{nl}} = \overline{P}^{\mathbf{q}=0,\mathrm{nl}}_{\alpha,\beta} = \int_{\rm cell} d^3r\,\rho^{\rm nl}_{\beta\mathbf{q}=0}(\mathbf{r})r_\alpha. \tag{72}$$

Again, this relation is generally applicable. For cubic symmetry, the Born effective charge tensor has only one independent element, which we write as $Z^{*}\equiv Z^{*\rm NG}_{\alpha\alpha}$. Of course, for the case of the noble gas atom "material," there is only one sublattice so the sum of the nonlocal contribution with the local part (including the ionic charge) will vanish due to the acoustic sum rule (ASR).[61]

For the case of the isolated noble gas atoms, we can use Eqs. (68) and (69) to relate the real-space octapole moment of $\rho^{\rm nl}_{\alpha\mathbf{q}=0}(\mathbf{r})$ [Fourier transform of Eq. (71)] averaged over the cell, to the second $\mathbf{q}$ derivative of $\overline{P}^{\mathbf{q},\mathrm{nl}}_{\alpha,\alpha}$ [see Eq. (C7)] evaluated at $\mathbf{q}=0$. Specifically, we should find that[15,17]

$$-\frac{1}{2}\frac{\partial^2\overline{P}^{\mathbf{q},\mathrm{nl,NG}}_{\alpha,\alpha}}{\partial q^2_\alpha}\bigg|_{\mathbf{q}=0} = \frac{1}{6\Omega}\int_{\rm cell} d^3r\,\rho^{\rm nl,NG}_{\alpha\mathbf{q}=0}(\mathbf{r})r^3_\alpha, \tag{73}$$

and similarly for the local part,

$$-\frac{1}{2}\frac{\partial^2\overline{P}^{\mathbf{q},\mathrm{loc,NG}}_{\alpha,\alpha}}{\partial q^2_\alpha}\bigg|_{\mathbf{q}=0} = \frac{1}{6\Omega}\int_{\rm cell} d^3r\left[-\nabla\cdot\mathbf{P}^{\rm loc,NG}_{\alpha\mathbf{q}=0}(\mathbf{r})\right]r^3_\alpha, \tag{74}$$

where we again perform the reciprocal space calculations using mixed electrical boundary conditions.

The comparisons in Eqs. (73) and (74) test both the long-wavelength expansion of the current operator (local and nonlocal), and the accuracy of the adiabatic first-order wavefunction at finite $\mathbf{q}$.

4. *Test of implementation: Longitudinal response*

To test $P^{\rm loc}_{\alpha,\alpha\mathbf{q}=0}$ and $\delta\psi^{\alpha}_{n\mathbf{k},\mathbf{q}=0}$, we calculate the first-order charge [left-hand side of Eq. (69)] from a $\mathbf{q}=0$ phonon by conventional DFPT, and compare to what we obtain for the right-hand side of Eq. (69) calculated using Eqs. (70) and (71) (with $\mathbf{q}=0$). We Fourier transform the quantities in Eq. (69) to real space and plot their

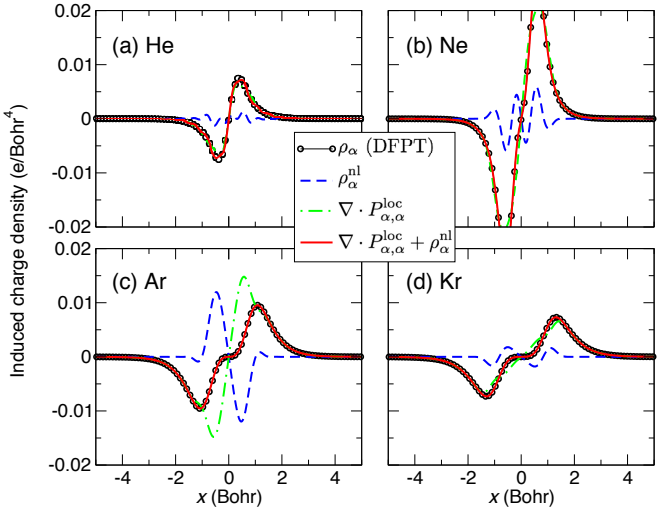

FIG. 1. (Color online) Planar average of the local [Eq. (70), green dot-dashed curve], nonlocal [Eq. (71), blue dashed], and total [Eq. (69), red solid] first-order charge for noble gas atoms displaced in the x direction by a $\mathbf{q}=0$ phonon. The black circles correspond to the first-order charge calculated using a conventional, static, DFPT calculation. The box size is $16\times16\times16$ Bohr, but zoomed in to only show ±5 Bohr.

planar averages in Fig. 1 for for He, Ne, Ar, and Kr atoms in $16\times16\times16$ Bohr cells. Summing the contributions from the nonlocal charge (blue dashed curves) and the gradients of the local induced polarization (green dot-dashed) gives the red solid curves in Fig. 1. As expected from Eq. (69), the red curve lies on top of the black circles, which correspond to the first-order charge from the $\mathbf{q}=0$ DFPT phonon calculations.

Now we can take the real-space moments of the curves in Fig. 1 and compare them with the results of our reciprocal space expansion. As discussed in the Sec. V A 3, the first moment of the blue dashed curves gives the nonlocal contribution to the Born effective charge, which should correspond to $\overline{P}^{\mathbf{q}=0,\mathrm{nl}}_{\alpha,\alpha}$ [Eq. (72)]. In Table II we give the nonlocal contribution to Z^{*} for the noble gas atoms in $14\times14\times14$ Bohr boxes. The ASR requires that the total Z^{*} vanishes; for our noble gas atoms, we calculate total Z^{*} less than 10^{-4} e, so the "local" part (including the contribution from the ionic charge) is the same magnitude but opposite sign as the numbers in the second and third columns of Table II.

The second column of Table II, labeled $P^{\rm nl}$, is calculated using the reciprocal space current and the third column (labeled $\rho^{\rm nl}$) is from the real-space dipole moment of the charge density. We see that there is excellent agreement between the two methods, indicating that $\overline{P}^{\mathbf{q}=0,\mathrm{nl}}_{\alpha,\alpha}$ is accurately calculated.

It is also clear from Fig. 1 and Table II that the nonlocal correction to the Born effective charge can be very large, on the order of one electron for Ar. We see a similarly large contribution for atoms with empty $3d$ shells (but projectors in this channel) such as a Ca atom or

TABLE II. Calculation of the Born effective charge and $\mu_{\rm L}$ using the moments of the local and nonlocal charge (columns labeled ρ) compared to the current-density implementation (columns labelled P) for atoms in a $14 \times 14 \times 14$ Bohr box. Mixed electrical boundary conditions are used.

	Z^* (e)		$\mu_{\rm L}$ (pC/m)			
	$P^{\rm nl}$	$\rho^{\rm nl}$	$P^{\rm loc}$	$\rho^{\rm loc}$	$P^{\rm nl}$	$\rho^{\rm nl}$
He	−0.027	−0.027	−0.470	−0.470	0.004	0.004
Ne	−0.155	−0.155	−1.872	−1.872	0.028	0.028
Ar	1.556	1.556	−4.620	−4.623	0.073	0.072
Kr	−0.214	−0.214	−5.878	−5.874	−0.099	−0.099

TABLE III. Longitudinal and shear (ICL and PM path) FxE coefficients for noble gas atoms in $14 \times 14 \times 14$ Bohr boxes, as well as the diamagnetic susceptibility, $\chi_{\rm mag}$ (ICL and PM path), and the quadrupole moment of the unperturbed charge density divided by two times the volume [*cf.* Eqs. (63) and (64)]. All quantities are in units of pC/m, and mixed electrical boundary conditions used.

	$\mu_{\rm L}$	$\mu_{\rm S}^{\rm ICL}$	$\mu_{\rm S}^{\rm PM}$	$\chi_{\rm mag}^{\rm ICL}$	$\chi_{\rm mag}^{\rm PM}$	$Q_{\rm NG}/2\Omega$
He	−0.468	−0.467	−0.464	−0.468	−0.464	−0.466
Ne	−1.840	−1.693	−1.655	−1.692	−1.655	−1.845
Ar	−4.545	−5.008	−5.086	−5.013	−5.081	−4.554
Kr	−5.968	−5.901	−5.917	−5.903	−5.921	−5.990

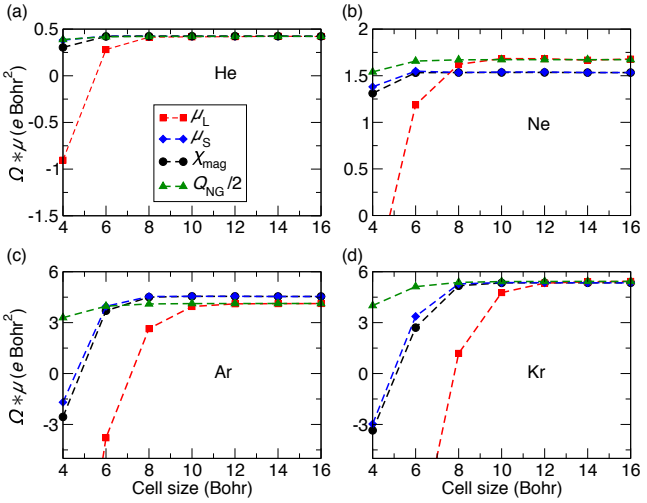

FIG. 2. (Color online) The longitudinal (red squares) and shear (blue diamonds) FxE coefficients, as well as the diamagnetic susceptibilities (black circles) and $Q_{\rm NG}/2\Omega$, for (a) He, (b) Ne, (c) Ar, and (d) Kr atoms in cells with various lattice constants. All quantities are multiplied by the cell volume, Ω.

Ti^{4+} ion (not shown).

Now we would like to test the accuracy of our long-wavelength expansion of the current operator (Sec. III C) for calculating $\mu_{\rm L}$. In Table II we give both the local and nonlocal contributions to $\mu_{\rm L}$ using the right-hand side of Eqs. (73) and (74) (labeled as $\rho^{\rm loc}$ and $\rho^{\rm nl}$), compared to those calculated from our current-density implementation [left-hand side of Eqs. (73) and (74), labeled as $P^{\rm loc}$ and $P^{\rm nl}$]. The agreement between the real-space moments and reciprocal-space derivatives of the expansion in Eq. (57) is excellent. Also, we can see that even though the nonlocal contribution to the Born effective charge is large for Ar, the first-order nonlocal charge is almost purely dipolar, with the the third moment being almost two orders of magnitude smaller than the contribution of the local part.

Also, from Table III and Fig. 2, we see that $\mu_{\rm L} = Q_{\rm NG}/2\Omega$ [consistent with Eq. (67)] quite accurately for sufficiently large simulation cells.

5. *Test of implementation: Shear response*

In Table III we give the longitudinal and shear FxE coefficients, as well as $\chi_{\rm mag}$ and $Q_{\rm NG}/2\Omega$, for noble gas atoms in $14 \times 14 \times 14$ Bohr boxes. For $\mu_{\rm S}$ and $\chi_{\rm mag}$, we give values using the ICL and PM paths for the nonlocal correction. In Fig. 2, we show the dependence of these quantities on the box size.

From Table III and Fig. 2, we see that $\mu_{\rm S} = \chi_{\rm mag}$ (consistent with the isotropic symmetry of the atoms) accurately for sufficiently large simulation cells. However, for atoms other than He, $\chi_{\rm mag}$ is noticeably different from $Q_{\rm NG}/2\Omega$, even for large box sizes. This discrepancy demonstrates that either Larmor's theorem or the Langevin theory of diamagnetism breaks down when nonlocal pseudopotentials are present (see Sec. VI for further discussion).

When we compare the two path choices, PM (Sec. III B 5) and ICL (Sec. III B 4), we find slight quantitative differences for the shear component and diamagnetic correction. However, the differences between the paths vanishes for $\mu_{\rm S}'$ [see Eq. (61)], indicating that although the dynamic contribution is path-dependent, the "true" shear response (which is vanishing for spherical symmetry) is not for this system. This result is an excellent test that our implementation is sound. Indeed, for a cubic solid, all three components of the electronic flexoelectric tensor $\boldsymbol{\mu}'$ can be related to the surface charge accummulated via the mechanical deformation of a finite crystallite; thus, they shouldn't depend on the aforementioned path choice. As the path choice is irrelevant in our context, in the next Section we shall perform our calculations on cubic oxides using the ICL path. In Sec. VI we shall provide a critical discussion of the ICL and PM prescriptions from a more general perspective, and leave a detailed comparison of the two approaches for a future work.

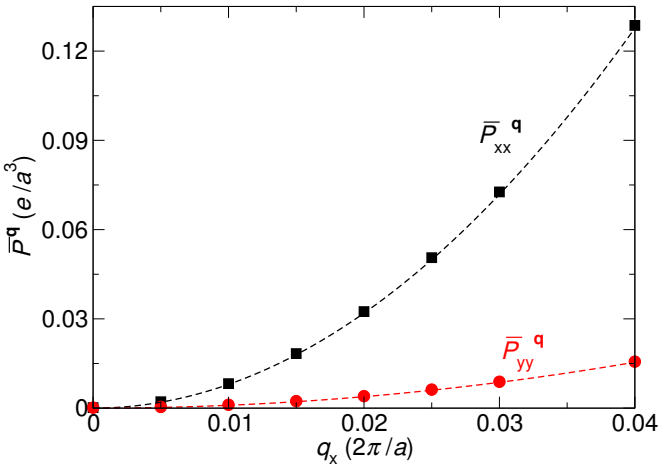

FIG. 3. (Color online) Induced polarization versus $\mathbf{q} = (q_x, 0, 0)$ for cubic $SrTiO_3$. The black (red) points correspond to the x (y) component of the polarization for atomic displacements of the atoms in the x (y) direction. Dashed curves are quadratic fits. Units are with respect to the calculated $SrTiO_3$ lattice constant $a = 7.435$ Bohr.

B. Cubic oxides

We now apply our methodology to calculate the bulk, clamped-ion FxE coefficients for several technologically important cubic oxides. As mentioned before, we will be using short circuit boundary conditions and the ICL path for the nonlocal correction.

As an example of a typical calculation, in Fig. 3 we plot the induced polarization [Eq. (57)] versus $\mathbf{q} = (q_x, 0, 0)$ for cubic $SrTiO_3$, both for polarization direction and atomic displacement $\alpha = \beta = x$ and $\alpha = \beta = y$. As expected, the dependence on q is quadratic (there is no linear term since cubic $SrTiO_3$ is not piezoelectric[15,17]), and $\overline{P}^{\mathbf{q}} = 0$ at $\mathbf{q} = 0$, which is required by the ASR condition that the sum of the Born effective charges should vanish.[61] By taking the second derivative of the black (red) dashed curves in Fig. 3, we can obtain $\mu^{\mathrm{I}}_{11,11}$ ($\mu^{\mathrm{I}}_{11,22}$). The remaining coefficient $\mu^{\mathrm{I}}_{12,12}$ is obtained by calculating $\overline{P}^{\mathbf{q}}_{12}$ at various $\mathbf{q} = (q_x, q_y, 0)$, and performing a numerical mixed derivative $\partial^2/\partial q_x \partial q_y$ (not shown).

In Table IV, we give the FxE coefficients corrected for the dynamic contribution [*cf.* Eq. (61)] and the RCC (Sec. IV C). As discussed above, the RCC is added to the longitudinal and transverse coefficients.[54] Note that the reported χ_{mag} is given in pC/m, whereas other quantities are in nC/m, so this correction is quite small for the materials calculated. The contribution of the nonlocal potentials to the FxE coefficients in Table IV, which are computed using the ICL path of Appendix C 1, represents a more significant correction than was the case in Sec. V A: they are in the range of 0.03 to 0.12 nC/m for the longitudinal and transverse coefficients, and in the range of -0.02 to 0.008 nC/m for the shear coefficients.

The only material for which first-principles calculations of the transverse and shear coefficients are available (in parentheses in Table IV) is $SrTiO_3$, and our values are in excellent agreement with those previous calculations.[18]

For all of the materials, the longitudinal and transverse responses are of similar magnitude, and the shear response is significantly smaller. This is a similar trend to that of the isolated noble gas atoms and of the IRC model [*cf.* Eq. (65)], suggesting that the response is dominated by the "spherical" contribution. The behavior of the cubic oxides differ significantly from the IRC model, however, when it comes to the contribution of the dynamic correction χ_{mag}. For isolated atoms, χ_{mag} is equal to $\mu_{\mathrm{IRC,S}}$, and is of the same order as $\mu'_{\mathrm{IRC,L}}$; therefore, a vanishing value of $\mu'_{\mathrm{IRC,S}}$ is only obtained after removing the dynamic contribution [Eq. (61)]. In the case of the cubic oxides, the dynamic correction is only a minor contribution to μ'_{S}, and χ_{mag} is two orders of magnitude smaller than μ'_{L}. In fact, χ_{mag} for the cubic oxides is comparable to that of the isolated atoms, while the FxE coefficients for the cubic oxides are two orders of magnitude larger. This indicates that although the bonding of atoms in the cubic compounds significantly enhances the FxE coefficients, it does not have a large effect on the dynamic correction.

It should be noted that the value of χ_{mag} for $SrTiO_3$ (-2.28×10^{-7} cm^3/g after unit conversion) is in fair agreement with the measured diamagnetic susceptibility of around -1×10^{-7} cm^3/g from Ref. 62.

VI. DISCUSSION

Before closing, it is useful to recap the technical issues that are associated with the calculation of the current density response in a nonlocal pseudopotential context, and critically discuss them in light of the result presented in this work. In particular, it is important to clarify whether our proposed approach matches the expectations, especially regarding the known transformation properties of the current density upon rototranslations, or whether there is any deviation that needs to be kept in mind when computing flexoelectric coefficients and other current-related linear-response properties.

As we have already discussed at length in the earlier Sections, our definition of the current density (i) satisfies the continuity equation by construction, (ii) correctly reduces to the textbook formula in region of space where the Hamiltonian is local, and (iii) is consistent with the known formula for the macroscopic current operator. However, we have not yet discussed some additional properties of the current density that were established in earlier works, that might be used as "sanity checks" of our implementation:

- Translational invariance: If the crystal undergoes a rigid translation with uniform velocity $\mathbf{v}$, the current density in the laboratory frame must be

$$\mathbf{J}(\mathbf{r}) = \mathbf{v}\rho(\mathbf{r}), \tag{75}$$

TABLE IV. Lattice constant, clamped-ion dielectric constant, rigid-core correction, and longitudinal, transverse, and shear clamped-ion FxE coefficients (under short circuit boundary conditions), as well as the diamagnetic susceptibility in units of nC/m. The FxE constants include the dynamic correction (Sec. III D) and RCC (Sec. IV C).

	a (Bohr)	ϵ	RCC	$\mu'_{\rm L}$	$\mu'_{\rm T}$	$\mu'_{\rm S}$	$\chi_{\rm mag}\times 10^3$
$SrTiO_3$	7.435	6.191	−0.049	−0.87 (−0.9[a],−0.88[b])	−0.84 (−0.83[b])	−0.08(−0.08[b])	−7.3
$BaTiO_3$	7.601	6.657	−0.107	−1.01 (−1.1[a])	−0.99	−0.08	−1.7
$SrZrO_3$	7.882	4.558	−0.049	−0.63	−0.58	−0.05	−36.0
$PbTiO_3$	7.496	8.370	−0.158	−1.39 (−1.5[a])	−1.35	−0.09	−22.4
MgO	8.058	3.148	−0.015	−0.28 (−0.3[a])	−0.30	−0.07	−66.1

[a] Ref. 17
[b] Ref. 18

where $\rho(\mathbf{r})$ is the static charge density.

- Larmor's theorem: The circulating currents generated in a crystallite by a uniform rotation with constant angular velocity $\boldsymbol{\omega}$ are, in the linear limit of small velocities, identical to the orbital currents that would be generated by an applied (and constant in time) **B**-field. As a corollary, the rotational g-factor of closed-shell molecules corresponds to their paramagnetic susceptibility.

- Langevin's diamagnetism: The magnetic susceptibility of a spherically symmetric atom is proportional to the quadrupolar moment of its ground-state charge density.

In the following, we shall analyze how our formalism stands in relationship to these latter "weak" [compared to the "strong" conditions (i-iii) above] criteria of validity. (By "weak" we mean sufficient for a physically sound calculation of the flexoelectric tensor, but possibly not enough for a wider range of physical properties.)

A. Translational invariance

Based on our results of Table III, we can safely conclude that both flavors of the current-density operator (ICL and PM) break translational invariance, Eq. (75). To see this, consider the shear flexoelectric coefficient of an isolated atom in a box, (e.g., $\mu_{\rm S,NG}$). This quantity can be defined in real space as the second moment of the microscopic current-density response to the displacement of an isolated atom,

$$\mu_{\rm S} = \frac{1}{2\Omega}\int d^3r \frac{\partial J_y(\mathbf{r})}{\partial \dot{\lambda}_y} x^2, \tag{76}$$

where $\dot{\lambda}_y$ stands for the velocity of the atom along y. This formula, as it stands, is not very practical for calculations: our implementation does not allow for a fully microscopic calculation of $\mathbf{J}(\mathbf{r})$, and therefore we had to replace Eq. (76) with computationally more tractable small-$\mathbf{q}$ expansions. Still, Eq. (76) is quite useful for our purposes, as it allows us to draw general conclusions about $\mathbf{J}(\mathbf{r})$ without the need for calculating it explicitly. In particular, if translational invariance Eq. (75) were true, Eq. (76) would imply that, e.g., $\mu_{\rm S,NG} = Q_{\rm NG}/2\Omega$. [This equality is a necessary but not sufficient condition for the validity of Eq. (75).] As we can see from Table III, $\mu_{\rm S,NG}$ is only approximately equal to $Q_{\rm NG}/2\Omega$ for both the ICL and PM flavors of the current-density operator. This implies that neither approach is able to guarantee translational invariance, Eq. (75). Similarly, the data we have in hand does not allow us to establish a clear preference between the PM and ICL recipes, as the discrepancies between the two are typically much smaller (and devoid of a systematic trend) than their respective failure at satisfying $\mu_{\rm S,NG} = Q_{\rm NG}/2\Omega$. Note that the discrepancy strictly consists of *solenoidal* (i.e., divergenceless) contributions to the current response; the longitudinal components are exactly treated, as one can verify from the excellent match between the longitudinal coefficient, $\mu_{\rm L}$, and the quadrupolar estimate in Table III.

B. Langevin diamagetism and Larmor's theorem

We come now to the assessment of the Larmor and Langevin results. One of the virtues of the PM recipe resides in its superior accuracy when comparing the orbital magnetic response to all-electron data. Indeed, in the context of our discussion, one can verify that it exactly complies with Langevin's theory of diamagnetism in the case of isolated spherical atoms.[63] The situation, however, is not so bright regarding Larmor's theorem. If the latter were satisfied, then the "rotational orbital susceptibility" $\chi_{\rm mag}$ would match Langevin's quadrupolar expression, as we know that Langevin's result holds in the case of a "true" **B**-field. By looking, again, at Table III, we clearly see that this is not the case – again, there is a discrepancy between the last column (based on the static quadrupole) and the calculated values of $\chi_{\rm mag}$. Since the deviations in $\chi_{\rm mag}$ and $\mu_{\rm S}$ are essentially identical in the limit of an isolated atom in a box, it is reasonable to assume that the underlying factors are similar.

It should be noted that our value for Ne (after unit conversion, ICL path) is $\chi^{\rm ICL}_{\rm mag} = -7.29\times10^{-6}$ cm^3/mole,

which is fairly close in magnitude to previously calculated values of the diamagnetic susceptibility of Ne: -7.75×10^{-6} cm^3/mole[31] and -7.79×10^{-6} cm^3/mole[33] (the sign is a matter of convention).

C. Unphysical charge transfer of nonlocal pseudopotentials

The reason why the current density violates both translational invariance and Larmor's theorem has to be sought in the unphysical transfer of charge between two distant points, $\mathbf{r}$ and $\mathbf{r}'$, that a nonlocal pseudopotential allows.

Taking the example of a single atom placed at $\mathbf{R} = 0$ and using the PM approach, it is shown in Appendix E that the current density can be written as

$$\mathbf{J}^{\mathrm{nl}}(\mathbf{r}) \sim \frac{\hat{\mathbf{r}} C(\hat{\mathbf{r}})}{r^2}. \tag{77}$$

where $C(\hat{\mathbf{r}})$ is a direction-dependent constant that depends on the nonlocal charge [Eq. (E5)]. Therefore, the current-density field diverges near the atomic site, $\mathbf{r} \to 0$, and such a divergence can have a different prefactor and sign depending on the direction.

A diverging $\mathbf{J}$-field is problematic to deal with and unphysical. One can easily realize that this characteristic is incompatible, for example, with the correct transformation laws of $\mathbf{J}$ under rigid translations. In particular, the electronic charge density is always finite in a vicinity of the nucleus, even in the all-electron case where the corresponding potential does, in fact, diverge. This implies that Eq. (75) cannot be satisfied by a diverging $\mathbf{J}$-field.

At present it is difficult to predict whether it might be possible to cure the above drawbacks by simply choosing a different path for the definition of the current operator, or whether these difficulties may require a deeper revision of the nonlocal pseudopotential theory in contexts where the microscopic current density is needed. In any case, the flexoelectric coefficients we calculated in this work for cubic materials are unaffected by these issues: Once the "diamagnetic" contribution has been removed, the three independent coefficients are all well defined in terms of the charge-density response. Nonetheless, the above caveats should be kept in mind when using the present current-density implementation to access flexoelectric coefficients in less symmetric materials, or other response properties that depend on the microscopic current response.

VII. CONCLUSIONS

We have developed a DFPT implementation for calculating the bulk clamped-ion flexoelectric tensor from a single unit cell. Therefore, we have overcome the limitations of previous implementations (Refs. 17 and 18), which required supercells to calculate the transverse and shear clamped-ion FxE coefficients.

Our implementation is based on calculating the microscopic current density resulting from the adiabatic displacement of a long-wavelength acoustic phonon. We have determined a form for the current-density operator that satisfies the continuity condition in the presence of nonlocal, norm-conserving pseudopotentials, and reduces to the correct form in the limit of a uniform, macroscopic perturbation, and/or when only local potentials are present.

In order to benchmark our methodology, we have used noble gas atoms to model systems of noninteracting spherical charge densities. The tests demonstrated the accuracy of our nonlocal correction to the current operator, as well as the calculated "dynamic" corrections derived in Ref. 20. For our form of the current density, we demonstrate that nonlocal pseudopotentials result in a violation of translational invariance and Larmor's theorem, though this does not affect our FxE coefficients after the dynamic contribution has been removed. Finally, we have applied our methodology to several cubic oxides, all of which show similar trends in that the longitudinal and transverse responses are similar (~ 1 nC/m), and the shear response is an order of magnitude smaller.

Combining the methodology of this paper with DFPT implementations for calculating the lattice-mediated contribution to the bulk FxE coefficients,[15,18] and the surface contribution,[18] will allow for efficient calculation of the full FxE response for a variety of materials.

ACKNOWLEDGMENTS

We are grateful to K. M. Rabe, D. R. Hamann, B. Monserrat, H. S. Kim, A. A. Schiaffino, and S. Y. Park for useful discussions. CED and DV were supported by ONR Grant N00014-16-1-2591. MS acknowledges funding from from the European Research Council (ERC) under the European Union's Horizon 2020 research and innovation programme (Grant Agreement No. 724529), and from MINECO-Spain through Grants No. FIS2013-48668-C2-2-P, MAT2016-77100-C2-2-P and SEV-2015-0496.

Appendix A: Essin *et al.* approach and the Ismail-Beigi, Chang, and Louie straight-line path

Here we demonstrate that the approach of Essin *et al.*[49] reduces to that of ICL.[31] We start from Eq. (45) and rewrite it as

$$\begin{aligned}\langle \mathbf{s}|\hat{\mathcal{J}}^{\mathrm{ICL}}_{\alpha}(\mathbf{q})|\mathbf{s}'\rangle &= -iH(\mathbf{s},\mathbf{s}')(s_\alpha - s'_\alpha)\frac{e^{-i\mathbf{q}\cdot\mathbf{s}} - e^{-i\mathbf{q}\cdot\mathbf{s}'}}{i\mathbf{q}\cdot(\mathbf{s}-\mathbf{s}')} \\ &= -i\left[\hat{r}_\alpha, \hat{H}\right]_{\mathbf{ss}'}\frac{e^{-i\mathbf{q}\cdot\mathbf{s}} - e^{-i\mathbf{q}\cdot\mathbf{s}'}}{i\mathbf{q}\cdot(\mathbf{s}-\mathbf{s}')} \\ &= -\left(i\left[\hat{r}_\alpha, \hat{T}\right]_{\mathbf{ss}'} + i\left[\hat{r}_\alpha, \hat{V}^{\mathrm{nl}}\right]_{\mathbf{ss}'}\right)\frac{e^{-i\mathbf{q}\cdot\mathbf{s}} - e^{-i\mathbf{q}\cdot\mathbf{s}'}}{i\mathbf{q}\cdot(\mathbf{s}-\mathbf{s}')},\end{aligned} \tag{A1}$$

where $\hat{T}$ is the kinetic energy operator and $\hat{V}^{\mathrm{nl}}$ is the nonlocal part of the potential (the local part of the potential does not contribute). We now factor out a $e^{-i\mathbf{q}\cdot\mathbf{s}'}$ and then expand the term outside of the parentheses

$$\langle \mathbf{s}|\hat{\mathcal{J}}^{\mathrm{ICL}}_{\alpha}(\mathbf{q})|\mathbf{s}'\rangle = -\left(i\left[\hat{r}_\alpha, \hat{T}\right]_{\mathbf{ss}'} + i\left[\hat{r}_\alpha, \hat{V}^{\mathrm{nl}}\right]_{\mathbf{ss}'}\right)e^{-i\mathbf{q}\cdot\mathbf{s}'}\left(-1 + \frac{i\mathbf{q}\cdot(\mathbf{s}-\mathbf{s}')}{2} + \frac{[\mathbf{q}\cdot(\mathbf{s}-\mathbf{s}')]^2}{6} + ...\right). \tag{A2}$$

As mentioned in Sec. III B 4, if $\mathbf{q} = 0$, then $\hat{\mathcal{J}}^{\mathrm{ICL}}_{\alpha}(\mathbf{q}=0) = i\left[\hat{r}_\alpha, \hat{H}\right] = -\hat{v}_\alpha$, the velocity operator.

Consider the case of a Hamiltonian with a local potential, so the only term in Eq. (A2) is the commutator of the position operator with the kinetic part of the Hamiltonian. We can rewrite this term as

$$\langle \mathbf{s}|\hat{\mathcal{J}}^{\mathrm{loc}}_{\alpha}(\mathbf{q})|\mathbf{s}'\rangle = -\left(-i\left[\hat{r}_\alpha, \hat{T}\right]_{\mathbf{ss}'} - \sum_{\gamma=1}^{3}\frac{q_\gamma}{2}\left[\hat{r}_\gamma, \left[\hat{r}_\alpha, \hat{T}\right]\right]_{\mathbf{ss}'} + \sum_{\gamma=1}^{3}\sum_{\xi=1}^{3}\frac{iq_\gamma q_\xi}{6}\left[\hat{r}_\xi, \left[\hat{r}_\gamma, \left[\hat{r}_\alpha, \hat{T}\right]\right]\right]_{\mathbf{ss}'} + ...\right)e^{-i\mathbf{q}\cdot\mathbf{s}'}. \tag{A3}$$

The term at zeroth order in q is simply the momentum operator: $\hat{p}_\alpha = -i\left[\hat{r}_\alpha, \hat{T}\right]$; at first order in q, we have $\hat{q}_\alpha/2$ (the nested commutator is simply the Kroneker delta function $-\delta_{\alpha\gamma}$); higher order terms vanish. So in the case of a Hamiltonian that only has a local potential,

$$\hat{\mathcal{J}}^{\mathbf{q},\mathrm{loc}}_{\alpha} = -\left(\hat{p}_\alpha + \frac{q_\alpha}{2}\right), \tag{A4}$$

which is the cell-periodic momentum operator for the case of local potentials, as we derive in Appendix B. Therefore the local and nonlocal components can be cleanly separated. The nonlocal part of the potential in Eq. A1 is addressed in Appendix C 1.

Note that the approach of Essin *et al.* does not work for an arbitrary choice of path. Specifically, if we were to use Eq. (42) with the PM path choice $\mathbf{s}' \to \mathbf{R} \to \mathbf{s}$, the expression would not reproduce the correct form of the current for local potentials (except for the case of the longitudinal response). Of course, in the PM form of the coupled Hamiltonian in Eq. (48), the current in the case of only local potentials trivially reduces to the correct form $\hat{\mathcal{J}}^{\mathrm{loc}}_{\alpha}(\mathbf{r}) = -\frac{1}{2}\left\{\hat{\rho}(\mathbf{r}), (\hat{p}_\alpha + \hat{A}_\alpha)\right\}$.

Appendix B: Derivation of induced polarization: Local potentials

In this section we derive $P^{\mathbf{q},\mathrm{loc}}_{\alpha,\kappa\beta}$ for Eq. (54). This is a straightforward generalization of what was derived by Umari, Dal Corso, and Resta[29] to finite $\mathbf{q}$ perturbations, and has been derived previously in other contexts (e.g. for determining magnetic[33] or dielectric[43] susceptibility, and in the context of phonon deformation potentials[64]).

Using the adiabatic expansion of the time-dependent wavefunction [Eqs. (10) and (11)], to first order in $\dot{\lambda}$ we can write the density matrix as

$$\rho(t) = -\frac{2}{N_k}\sum_{n\mathbf{k}}|\Psi_{n\mathbf{k}}[\lambda(t)]\rangle\langle\Psi_{n\mathbf{k}}[\lambda(t)]| \simeq -\frac{2}{N_k}\sum_{n\mathbf{k}}\left[|\psi_{n\mathbf{k}}\rangle\langle\psi_{n\mathbf{k}}| + \dot{\lambda}(|\delta\psi_{n\mathbf{k}}\rangle\langle\psi_{n\mathbf{k}}| + |\psi_{n\mathbf{k}}\rangle\langle\delta\psi_{n\mathbf{k}}|)\right] \tag{B1}$$

where the factor of two is assuming spin degeneracy. If we apply the local current-density operator [Eq. (29)], retaining terms only to linear order in $\dot{\lambda}$, and take the derivative with respect to $\dot{\lambda}$ we obtain the induced polarization

$$P^{\mathrm{loc}}_{\alpha}(\mathbf{r}) = -\frac{1}{N_k}\sum_{n\mathbf{k}}\left[\langle\psi_{n\mathbf{k}}|\mathbf{r}\rangle\langle\mathbf{r}|\hat{p}_\alpha|\delta\psi_{n\mathbf{k}}\rangle + \langle\delta\psi_{n\mathbf{k}}|\mathbf{r}\rangle\langle\mathbf{r}|\hat{p}_\alpha|\psi_{n\mathbf{k}}\rangle + \langle\psi_{n\mathbf{k}}|\hat{p}_\alpha|\mathbf{r}\rangle\langle\mathbf{r}|\delta\psi_{n\mathbf{k}}\rangle + \langle\delta\psi_{n\mathbf{k}}|\hat{p}_\alpha|\mathbf{r}\rangle\langle\mathbf{r}|\psi_{n\mathbf{k}}\rangle\right]. \tag{B2}$$

Now consider the perturbation in Eq. (3): the displacement of a sublattice κ in direction β modulated by a phase with wavevector $\mathbf{q}$. We begin with the real-space expression for the polarization induced by this perturbation:

$$P^{\mathbf{q},\mathrm{loc}}_{\alpha,\kappa\beta}(\mathbf{r}) = -\frac{1}{N_k}\sum_{n\mathbf{k}}\Big[\langle\psi_{n\mathbf{k}}|\mathbf{r}\rangle\langle\mathbf{r}|\hat{p}_\alpha|\delta\psi^{\kappa\beta}_{n\mathbf{k},\mathbf{q}}\rangle + \langle\delta\psi^{\kappa\beta}_{n\mathbf{k},-\mathbf{q}}|\mathbf{r}\rangle\langle\mathbf{r}|\hat{p}_\alpha|\psi_{n\mathbf{k}}\rangle + \langle\psi_{n\mathbf{k}}|\hat{p}_\alpha|\mathbf{r}\rangle\langle\mathbf{r}|\delta\psi^{\kappa\beta}_{n\mathbf{k},\mathbf{q}}\rangle + \langle\delta\psi^{\kappa\beta}_{n\mathbf{k},-\mathbf{q}}|\hat{p}_\alpha|\mathbf{r}\rangle\langle\mathbf{r}|\psi_{n\mathbf{k}}\rangle\Big] \tag{B3}$$

where the subscript $\mathbf{q}$ in $\delta\psi^{\kappa\beta}_{n\mathbf{k},\pm\mathbf{q}}$ indicates that the perturbation couples states at $\mathbf{k}$ to those at $\mathbf{k}\pm\mathbf{q}$. If we assume TRS [see Eq. (25)], then we have

$$P^{\mathbf{q},\mathrm{loc}}_{\alpha,\kappa\beta}(\mathbf{r}) = -\frac{2}{N_k}\sum_{n\mathbf{k}}\Big[\langle\psi_{n\mathbf{k}}|\mathbf{r}\rangle\langle\mathbf{r}|\hat{p}_\alpha|\delta\psi^{\kappa\beta}_{n\mathbf{k},\mathbf{q}}\rangle + \langle\psi_{n\mathbf{k}}|\hat{p}_\alpha|\mathbf{r}\rangle\langle\mathbf{r}|\delta\psi^{\kappa\beta}_{n\mathbf{k},\mathbf{q}}\rangle\Big] \tag{B4}$$

We Fourier transform Eq. (B4) to reciprocal space and consider the cell periodic part

$$P^{\mathrm{loc}}_{\alpha,\kappa\beta}(\mathbf{G}+\mathbf{q}) = -\frac{2}{N_k}\sum_{n\mathbf{k}}\int d^3r\Big[\langle\psi_{n\mathbf{k}}|\mathbf{r}\rangle e^{-i(\mathbf{G}+\mathbf{q})\cdot\mathbf{r}}\langle\mathbf{r}|\hat{p}_\alpha|\delta\psi^{\kappa\beta}_{n\mathbf{k},\mathbf{q}}\rangle + \langle\psi_{n\mathbf{k}}|\hat{p}_\alpha|\mathbf{r}\rangle e^{-i(\mathbf{G}+\mathbf{q})\cdot\mathbf{r}}\langle\mathbf{r}|\delta\psi^{\kappa\beta}_{n\mathbf{k},\mathbf{q}}\rangle\Big] \tag{B5}$$

We now explicitly insert the expansion of the wavefunctions in terms of plane waves

$$\begin{aligned}\psi_{\mathbf{k}}(\mathbf{s}) &= \sum_m c_{\mathbf{k},\mathbf{G}_m} e^{i(\mathbf{G}_m+\mathbf{k})\cdot\mathbf{s}}\\ \delta\psi^{\kappa\beta}_{n\mathbf{k},\mathbf{q}}(\mathbf{s}) &= \sum_m \delta c_{\mathbf{k}+\mathbf{q},\mathbf{G}_m} e^{i(\mathbf{G}_m+\mathbf{k}+\mathbf{q})\cdot\mathbf{s}},\end{aligned} \tag{B6}$$

where we have dropped the band index and the $\kappa\beta$ indicies for the expansion coefficients c and δc, and m indexes a reciprocal lattice vector $\mathbf{G}_m$. Then, applying the momentum operator,

$$\begin{aligned}P^{\mathrm{loc}}_{\alpha,\kappa\beta}(\mathbf{G}+\mathbf{q}) &= -\frac{2}{N_k}\sum_{\mathbf{k}}\sum_{m,m'}\int d^3r c^*_{\mathbf{k},\mathbf{G}_m}\delta c_{\mathbf{k}+q_\alpha,\mathbf{G}_{m'}}\Big[(k_\alpha+q_\alpha+G_{\alpha,m'})e^{-i(\mathbf{G}+\mathbf{G}_m-\mathbf{G}_{m'})\cdot\mathbf{r}}\\ &\qquad + (k_\alpha+G_{\alpha,m})e^{-i(\mathbf{G}+\mathbf{G}_m-\mathbf{G}_{m'})\cdot\mathbf{r}}\Big]\\ &= -\frac{4}{N_k}\sum_{\mathbf{k}}\sum_m c^*_{\mathbf{k},\mathbf{G}_m}\delta c_{\mathbf{k}+q_\alpha,\mathbf{G}_m+\mathbf{G}}\left(k_\alpha+G_{\alpha,m}+\frac{q_\alpha+G_\alpha}{2}\right)\\ &= -\frac{2}{N_k}\sum_{n\mathbf{k}}\langle u_{n\mathbf{k}}|e^{i\mathbf{G}\cdot\hat{\mathbf{r}}}\left(\hat{p}^{\mathbf{k}}_\alpha+\frac{q_\alpha}{2}\right)+\left(\hat{p}^{\mathbf{k}}_\alpha+\frac{q_\alpha}{2}\right)e^{i\mathbf{G}\cdot\hat{\mathbf{r}}}|\delta u^{\kappa\beta}_{n\mathbf{k},\mathbf{q}}\rangle,\end{aligned} \tag{B7}$$

where, in the last line, we have restored the band and $\kappa\beta$ indices, $\hat{p}^{\mathbf{k}}_\alpha = -i\hat{\nabla}_\alpha + k_\alpha$ is the cell-periodic momentum operator ($\hat{\nabla}_\alpha$ is a spatial derivative in the α direction), and we have used that $\psi_{n\mathbf{k}}(\mathbf{s}) = u_{n\mathbf{k}}(\mathbf{s})e^{i\mathbf{k}\cdot\mathbf{s}}$. In Sec. V A, we use this result to calculate real-space moments of the local contribution to the FxE coefficient. Otherwise, we are usually interested in the $\mathbf{G}=0$ term:

$$\overline{P}^{\mathbf{q},\mathrm{loc}}_{\alpha,\kappa\beta} = -\frac{4}{N_k}\sum_{n\mathbf{k}}\langle u_{n\mathbf{k}}|\left(\hat{p}^{\mathbf{k}}_\alpha+\frac{q_\alpha}{2}\right)|\delta u^{\kappa\beta}_{n\mathbf{k},\mathbf{q}}\rangle. \tag{B8}$$

Appendix C: Current density in the presence of nonlocal pseudopotentials

Here we derive the expansion in $\mathbf{q}$ of the contributions to the current from the nonlocal potentials [$P^{\mathbf{q},\mathrm{nl}}_{\alpha,\kappa\beta}$ in Eq. (54)]. The nonlocal potential that we are interested in is that of the norm-conserving pseudopotential. In reciprocal space, the nonlocal potential in the seperable Kleinman-Bylander[27] form is given by[65]

$$V^{\mathrm{nl}}(\mathbf{K},\mathbf{K}') = \sum_\zeta e^{-i\mathbf{K}\cdot\mathbf{R}_\zeta}\left(\sum_{lm}\frac{Y^*_{\zeta lm}(\hat{\mathbf{K}})T^*_{\zeta l}(|\mathbf{K}|)\times T_{\zeta l}(|\mathbf{K}'|)Y_{\zeta lm}(\hat{\mathbf{K}}')}{E^{\mathrm{KB}}_{\zeta l}}\right)e^{i\mathbf{K}'\cdot\mathbf{R}_\zeta} \tag{C1}$$

where $\mathbf{K}=\mathbf{G}+\mathbf{k}$; $\mathbf{R}_\zeta$ is the atomic position of atom ζ; $Y_{\zeta lm}$ is the spherical harmonic for the lm angular momentum channel; $T_{\zeta l}(K)$ is the Fourier transform of the radial function, $\widetilde{\psi}_{\zeta l}(r)V_{\zeta l}(r)$, where $V_{\zeta l}(r)$ are the pseudopotentials

and $\widetilde{\psi}_{\zeta l}(r)$ the pseudoorbitals; $E^{\rm KB}_{\zeta l} = \langle \widetilde{\psi}_{\zeta l}|\hat{V}_l|\widetilde{\psi}_{\zeta l}\rangle$ is the Kleinman-Bylander energies. The term in the parentheses is the nonlocal form factor, and the phase factors surrounding it are the structure factors. We define

$$\langle \mathbf{K}|\phi_{\zeta lm}\rangle = e^{i\mathbf{K}\cdot\mathbf{R}_\zeta} Y_{\zeta lm}(\hat{\mathbf{K}}) T_{\zeta l}(|\mathbf{K}|) \tag{C2}$$

so

$$\hat{V}^{\rm nl} = \sum_{\zeta lm} \frac{|\phi_{\zeta lm}\rangle\langle\phi_{\zeta lm}|}{E^{\rm KB}_{\zeta l}}. \tag{C3}$$

1. Ismail-Beigi, Chang, and Louie straight-line path

For the straight-line ICL path of Essin *et al.*[49] and Ismail-Beigi, Chang, and Louie,[31] we combine Eq. (46) and (assuming we have TRS) Eq. (26). Since we have already addressed the local part in Appendix B, we only consider the nonlocal part of the Hamiltonian, defining the operator

$$\langle \mathbf{s}|\hat{\mathcal{J}}^{\mathbf{k},\mathbf{q},\rm ICL,nl}_\alpha|\mathbf{s}'\rangle = -iV^{\mathbf{k},\rm nl}(\mathbf{s},\mathbf{s}')(s_\alpha - s'_\alpha)\left[\frac{e^{-i\mathbf{q}\cdot(\mathbf{s}-\mathbf{s}')}-1}{i\mathbf{q}\cdot(\mathbf{s}-\mathbf{s}')}\right]. \tag{C4}$$

Expanding the term in square brackets in powers of $\mathbf{q}$ gives

$$\begin{aligned}\langle \mathbf{s}|\hat{\mathcal{J}}^{\mathbf{k},\mathbf{q},\rm ICL,nl}_\alpha|\mathbf{s}'\rangle &= iV^{\mathbf{k},\rm nl}(\mathbf{s},\mathbf{s}')(s_\alpha - s'_\alpha)\left[1 - \frac{i\mathbf{q}\cdot(\mathbf{s}-\mathbf{s}')}{2} + \frac{[i\mathbf{q}\cdot(\mathbf{s}-\mathbf{s}')]^2}{6} - \cdots\right]. \\ &= i\left[\hat{r}_\alpha, \hat{V}^{\mathbf{k},\rm nl}\right]_{\mathbf{s}\mathbf{s}'} - \frac{1}{2}\sum_{\gamma=1}^{3} q_\gamma \left[\hat{r}_\gamma, \left[\hat{r}_\alpha, \hat{V}^{\mathbf{k},\rm nl}\right]\right]_{\mathbf{s}\mathbf{s}'} - \frac{i}{6}\sum_{\gamma=1}^{3}\sum_{\xi=1}^{3} q_\gamma q_\xi \left[\hat{r}_\xi, \left[\hat{r}_\gamma, \left[\hat{r}_\alpha, \hat{V}^{\mathbf{k},\rm nl}\right]\right]\right]_{\mathbf{s}\mathbf{s}'} + \cdots,\end{aligned} \tag{C5}$$

so we can write the operator as

$$\hat{\mathcal{J}}^{\mathbf{k},\mathbf{q},\rm ICL,nl}_\alpha = \sum_{\gamma_1\cdots\gamma_n} \frac{q_{\gamma_1}\cdots q_{\gamma_n}}{(n+1)!} \frac{\partial^{n+1}\hat{V}^{\mathbf{k},\rm nl}}{\partial k_\alpha \partial k_{\gamma_1}\cdots\partial k_{\gamma_n}}. \tag{C6}$$

Plugging Eq. (C6) (and only retaining terms in $\hat{\mathcal{J}}^{\mathbf{k},\mathbf{q},\rm ICL,nl}_\alpha$ to second order in $\mathbf{q}$) into Eq. (21) gives

$$\overline{P}^{\mathbf{q},\rm ICL,nl}_{\alpha,\kappa\beta} \simeq -\frac{4}{N_k}\sum_{n\mathbf{k}}\left[\langle u_{n\mathbf{k}}|\frac{\partial\hat{V}^{\mathbf{k},\rm nl}}{\partial k_\alpha}|\delta u^{\kappa\beta}_{n\mathbf{k},\mathbf{q}}\rangle + \frac{1}{2}\sum_{\gamma=1}^{3} q_\gamma \langle u_{n\mathbf{k}}|\frac{\partial^2\hat{V}^{\mathbf{k},\rm nl}}{\partial k_\alpha \partial k_\gamma}|\delta u^{\kappa\beta}_{n\mathbf{k},\mathbf{q}}\rangle + \frac{1}{6}\sum_{\gamma=1}^{3}\sum_{\xi=1}^{3} q_\gamma q_\xi \langle u_{n\mathbf{k}}|\frac{\partial^3\hat{V}^{\mathbf{k},\rm nl}}{\partial k_\alpha\partial k_\gamma\partial k_\xi}|\delta u^{\kappa\beta}_{n\mathbf{k},\mathbf{q}}\rangle\right], \tag{C7}$$

where, in terms of the cell-periodic projectors $\phi^{\mathbf{k}}_{\zeta lm}(\mathbf{s}) = e^{-i\mathbf{k}\cdot\mathbf{s}}\phi_{\zeta lm}(\mathbf{s})$ [see Eq. (C3)], the derivatives of the nonlocal potential operator are

$$\frac{\partial\hat{V}^{\mathbf{k},\rm nl}}{\partial k_\alpha} = \sum_{\zeta lm}\frac{1}{E^{\rm KB}_{\zeta l}}\left(|\phi^{\mathbf{k}}_{\zeta lm}\rangle\langle\partial_\alpha\phi^{\mathbf{k}}_{\zeta lm}| + |\partial_\alpha\phi^{\mathbf{k}}_{\zeta lm}\rangle\langle\phi^{\mathbf{k}}_{\zeta lm}|\right), \tag{C8}$$

$$\frac{\partial^2\hat{V}^{\mathbf{k},\rm nl}}{\partial k_\alpha\partial k_\gamma} = \sum_{\zeta lm}\frac{1}{E^{\rm KB}_{\zeta l}}\left(|\partial_\gamma\phi^{\mathbf{k}}_{\zeta lm}\rangle\langle\partial_\alpha\phi^{\mathbf{k}}_{\zeta lm}| + |\phi^{\mathbf{k}}_{\zeta lm}\rangle\langle\partial_\alpha\partial_\gamma\phi^{\mathbf{k}}_{\zeta lm}| + |\partial_\alpha\partial_\gamma\phi^{\mathbf{k}}_{\zeta lm}\rangle\langle\phi^{\mathbf{k}}_{\zeta lm}| + |\partial_\alpha\phi^{\mathbf{k}}_{\zeta lm}\rangle\langle\partial_\gamma\phi^{\mathbf{k}}_{\zeta lm}|\right), \tag{C9}$$

and

$$\begin{aligned}\frac{\partial^3\hat{V}^{\mathbf{k},\rm nl}}{\partial k_\alpha\partial k_\gamma\partial k_\xi} = \sum_{\zeta lm}\frac{1}{E^{\rm KB}_{\zeta l}}\big(&|\partial_\xi\partial_\gamma\phi^{\mathbf{k}}_{\zeta lm}\rangle\langle\partial_\alpha\phi^{\mathbf{k}}_{\zeta lm}| + |\partial_\xi\phi^{\mathbf{k}}_{\zeta lm}\rangle\langle\partial_\gamma\partial_\alpha\phi^{\mathbf{k}}_{\zeta lm}| + |\partial_\gamma\phi^{\mathbf{k}}_{\zeta lm}\rangle\langle\partial_\alpha\partial_\xi\phi^{\mathbf{k}}_{\zeta lm}| + \langle u_{n\mathbf{k}}|\phi^{\mathbf{k}}_{\zeta lm}\rangle\langle\partial_\gamma\partial_\alpha\partial_\xi\phi^{\mathbf{k}}_{\zeta lm}| \\ &+ |\partial_\gamma\partial_\alpha\partial_\xi\phi^{\mathbf{k}}_{\zeta lm}\rangle\langle\phi^{\mathbf{k}}_{\zeta lm}| + \langle u_{n\mathbf{k}}|\partial_\alpha\partial_\xi\phi^{\mathbf{k}}_{\zeta lm}\rangle\langle\partial_\gamma\phi^{\mathbf{k}}_{\zeta lm}| + |\partial_\gamma\partial_\alpha\phi^{\mathbf{k}}_{\zeta lm}\rangle\langle\partial_\xi\phi^{\mathbf{k}}_{\zeta lm}| + |\partial_\alpha\phi^{\mathbf{k}}_{\zeta lm}\rangle\langle\partial_\gamma\partial_\xi\phi^{\mathbf{k}}_{\zeta lm}|\big).\end{aligned} \tag{C10}$$

The three terms in Eq. (C7) correspond to last three terms in Eq. (53) for the ICL path. The first term in Eq. (C7) represents the well-known nonlocal correction to the Born effective charge (with an overall negative sign from the electron charge), which, combined with the local part [Eq. (B8)] gives that the velocity operator $\hat{v}^{\mathbf{k},\mathbf{q}}_\alpha$ and should be the same for either path choice.

2. Pickard and Mauri path through atom center

The PM[32] path goes through the center of the atom. For simplicity of the derivation, we consider a single atom positioned at the origin ($\mathbf{R} = 0$); the generalization to an atom not at the origin simply involves an extra phase in the structure factors in Eq. (C1). Then Eq. (51) becomes

$$\langle \mathbf{s}|\hat{\mathcal{J}}_\alpha^{\mathrm{PM,nl}}(\mathbf{q})|\mathbf{s}'\rangle = -iV^{\mathrm{nl}}(\mathbf{s},\mathbf{s}')\left[s'_\alpha \frac{1-e^{-i\mathbf{q}\cdot\mathbf{s}'}}{i\mathbf{q}\cdot\mathbf{s}'} + s_\alpha \frac{e^{-i\mathbf{q}\cdot\mathbf{s}}-1}{i\mathbf{q}\cdot\mathbf{s}}\right]. \tag{C11}$$

Following the same steps as in Appendix C 1, we arrive a similar expression to Eq. (C7),

$$\overline{P}^{\mathbf{q},\mathrm{ICL,nl}}_{\alpha,\kappa\beta} \simeq -\frac{4}{N_k}\sum_{n\mathbf{k}}\left[\langle u_{n\mathbf{k}}|\frac{\partial \hat{V}^{\mathbf{k},\mathrm{nl}}}{\partial k_\alpha}|\delta u^{\kappa\beta}_{n\mathbf{k},\mathbf{q}}\rangle + \frac{1}{2}\sum_{\gamma=1}^{3} q_\gamma \langle u_{n\mathbf{k}}|\hat{V}^{\mathbf{k},\mathrm{nl}(1)}_{\alpha\gamma}|\delta u^{\kappa\beta}_{n\mathbf{k},\mathbf{q}}\rangle + \frac{1}{6}\sum_{\gamma=1}^{3}\sum_{\xi=1}^{3} q_\gamma q_\xi \langle u_{n\mathbf{k}}|\hat{V}^{\mathbf{k},\mathrm{nl}(2)}_{\alpha\gamma\xi}|\delta u^{\kappa\beta}_{n\mathbf{k},\mathbf{q}}\rangle\right], \tag{C12}$$

with slightly different operators for the terms to first and second order in $\mathbf{q}$ (the zeroth order term is the same as for the ICL path, as expected). At "first" order:

$$\hat{V}^{\mathbf{k},\mathrm{nl}(1)}_{\alpha\gamma} = \sum_{\zeta lm}\frac{1}{E^{\mathrm{KB}}_{\zeta l}}\big(2|\partial_\alpha\phi^{\mathbf{k}}_{\zeta lm}\rangle\langle\partial_\gamma\phi^{\mathbf{k}}_{\zeta lm}| + |\phi^{\mathbf{k}}_{\zeta lm}\rangle\langle\partial_\alpha\partial_\gamma\phi^{\mathbf{k}}_{\zeta lm}| + |\partial_\alpha\partial_\gamma\phi^{\mathbf{k}}_{\zeta lm}\rangle\langle\phi^{\mathbf{k}}_{\zeta lm}|\big). \tag{C13}$$

We see immediately that for the case of a longitudinal perturbation, this is identical to the ICL path [*cf.* Eq. (C9)]. At "second" order

$$\hat{V}^{\mathbf{k},\mathrm{nl}(2)}_{\alpha\gamma\xi} = \sum_{\zeta lm}\frac{1}{E^{\mathrm{KB}}_{\zeta l}}\big(3|\partial_\alpha\partial_\gamma\phi^{\mathbf{k}}_{\zeta lm}\rangle\langle\partial_\xi\phi^{\mathbf{k}}_{\zeta lm}| + 3|\partial_\alpha\phi^{\mathbf{k}}_{\zeta lm}\rangle\langle\partial_\gamma\partial_\xi\phi^{\mathbf{k}}_{\zeta lm}| + |\phi^{\mathbf{k}}_{\zeta lm}\rangle\langle\partial_\alpha\partial_\gamma\partial_\xi\phi^{\mathbf{k}}_{\zeta lm}| + |\partial_\alpha\partial_\gamma\partial_\xi\phi^{\mathbf{k}}_{\zeta lm}\rangle\langle\phi^{\mathbf{k}}_{\zeta lm}|\big). \tag{C14}$$

Once again, this term is the same as for the ICL path for longitudinal perturbations [*cf.* Eq. (C10)].

Appendix D: Diamagnetic correction

In this section we provide some details about the calculation of the dynamic contribution to the transverse and shear FxE coefficients, which is related to the diamagnetic susceptibility. We refer the reader to Ref. 20 for a complete discussion.

For the case of a small deformation $\mathbf{u}$ that is applied to the atoms of a crystal adiabatically through the perturbation parameter $\lambda(t)$, the dynamic contribution to linear order in the velocity is

$$\dot{\lambda}\hat{H}^{(\dot{\lambda})} = -\frac{1}{2}\left(\hat{\mathbf{A}}\cdot\hat{\mathbf{p}} + \hat{\mathbf{p}}\cdot\hat{\mathbf{A}}\right). \tag{D1}$$

Here $\mathbf{A}$ is not the vector potential of electromagnetism, but one that emerges when transforming from the static reference frame to the dynamic one. For a monochromatic perturbation, it becomes just $\mathbf{A} = \dot{\lambda}\mathbf{u} = \dot{\lambda}e^{i\mathbf{q}\cdot\mathbf{r}}$, so

$$\hat{H}^{(\dot{\lambda}_\beta)}(\mathbf{q}) = -e^{i\mathbf{q}\cdot\hat{\mathbf{r}}}\left(\hat{p}_\beta + \frac{q_\beta}{2}\right) \tag{D2}$$

which we recognize as the local current operator [*cf.* Eq. (A4) or (B8)]. Therefore, the first-order, cell-periodic wavefunctions with respect to this perturbation are

$$|\partial_{\dot{\lambda}_\beta} u^\beta_{n\mathbf{k},\mathbf{q}}\rangle = \sum_m^{\mathrm{unocc}} \frac{|u_{m\mathbf{k},\mathbf{q}}\rangle\langle u_{m\mathbf{k},\mathbf{q}}|\left(\hat{p}^{\mathbf{k}}_\beta + q_\beta/2\right)|u_{n\mathbf{k}}\rangle}{\epsilon_{m\mathbf{k},\mathbf{q}} - \epsilon_{n\mathbf{k}}}, \tag{D3}$$

and the (cell averaged) induced polarization from the dynamic part of the metric perturbation is

$$\overline{P}^{\mathbf{q},\,\mathrm{dyn}}_{\alpha,\beta} = \frac{2}{N_k}\sum_{n\mathbf{k}}\Big(\langle u_{n\mathbf{k}}|\hat{\mathcal{J}}^{\mathbf{k},\mathbf{q}}_\alpha|\partial_{\dot{\lambda}_\beta}u^\beta_{n\mathbf{k},\mathbf{q}}\rangle + \langle\partial_{\dot{\lambda}_\beta}u^\beta_{n\mathbf{k},-\mathbf{q}}|\hat{\mathcal{J}}^{\mathbf{k},-\mathbf{q}}_\alpha|u_{n\mathbf{k}}\rangle\Big). \tag{D4}$$

The contribution to the FxE coefficient is determined by taking the second derivative of $\overline{P}^{\mathbf{q},\mathrm{dyn}}_{\alpha,\beta}$ with respect to q:

$$\overline{P}^{(2,\omega\nu),\ \mathrm{dyn}}_{\alpha,\beta} = \left.\frac{\partial^2 \overline{P}^{\mathbf{q},\mathrm{dyn}}_{\alpha,\beta}}{\partial q_\omega \partial q_\nu}\right|_{\mathbf{q}=0}. \tag{D5}$$

The dynamic contribution is closely related to the diamagnetic susceptibility, $\chi_{\alpha\beta}$. In fact, in the case where only local potentials are present in the Hamiltonian [so $\hat{\mathcal{J}}^{\mathbf{k},\mathbf{q}}_\beta = \hat{p}^{\mathbf{k}}_\beta + q_\beta/2$ in Eq. (D4)], Eq. (D5) has the same form as the expressions for the magnetic susceptibility derived in, e.g., Refs. 30 and 33 [*cf.* Eq. (11) and Eq. (9) in those works, respectively].

The magnetic susceptibility relates the magnetization, M to the external magnetic field B via $M_\gamma = \chi^{\mathrm{mag}}_{\gamma\lambda} B_\lambda$. This can be rewritten to relate the bound currents to the vector potential:

$$J_\alpha = \epsilon^{\alpha\zeta\gamma} \nabla_\zeta \chi_{\gamma\lambda} \epsilon^{\lambda\rho\beta} \nabla_\rho A_\beta, \tag{D6}$$

so that

$$\overline{P}^{\mathbf{q},\ \mathrm{dyn}}_{\alpha,\beta} \sim \epsilon^{\alpha\zeta\gamma} q_\zeta \chi_{\gamma\lambda} \epsilon^{\beta\lambda\rho} q_\rho, \tag{D7}$$

where we have expressed the spatial derivatives in reciprocal space and canceled the resulting negative sign by permutating the second Levi-Civita symbol. Performing the q derivatives in Eq. (D5) gives

$$\overline{P}^{(2,\omega\nu),\ \mathrm{dyn}}_{\alpha,\beta} = \sum_{\gamma\lambda} \left(\epsilon^{\alpha\omega\gamma}\epsilon^{\beta\lambda\nu} + \epsilon^{\alpha\nu\gamma}\epsilon^{\beta\lambda\omega}\right) \chi_{\gamma\lambda}. \tag{D8}$$

In the case that nonlocal potentials are present in the Hamiltonian, a calculation of the magnetic susceptibility would involve replacing $\left(\hat{p}^{\mathbf{k}}_\beta + q_\beta/2\right)$ in Eq. (D3) with the full current operator from Eq. (53), as well as evaluating an extra term originating from the second order Hamiltonian.[31,32,35] This is in contrast to the case of the dynamic contribution we would like to calculate, where the only change in the case of nonlocal potentials is replacing $\left(\hat{p}^{\mathbf{k}}_\beta + q_\beta/2\right)$ in Eq. (D3) with the full current operator from Eq. (53); Eqs. (D2) and (D3) are unchanged. Therefore, Eq. (D4) does not strictly correspond to the magnetic susceptibility in this case. However, we show in Sec. VI that the numerical values are quite similar to previously calculated diamagnetic susceptibilities .

Appendix E: Divergence of the current at the atomic site for the PM path

To illustrate the point that nonlocal pseudopotentials allow unphysical transfer of charge between $\mathbf{r}$ and $\mathbf{r}'$, we shall consider the PM[32] definition of the current density, which provides a particularly transparent manifestation of such unphysical behavior. For simplicity, we focus our attention on a single atomic sphere [so we drop the ζ index of Eq. (48)], and we set the corresponding nuclear site as the coordinate origin. (There is no approximation here, as the contributions from different sites are spatially separated and additive.) Now suppose we wish to evaluate the nonlocal current density at the point $\mathbf{r}_0$. We need then to calculate Eq. (39) with Eq. (48), using a Dirac delta as a vector potential,

$$\mathbf{A}(\mathbf{r}) = A\hat{\mathbf{r}}_0\, \delta(\mathbf{r} - \mathbf{r}_0), \tag{E1}$$

where the caret above the position variable denotes a direction (not to be confused with the position operator). We choose it to be oriented along the radial direction, as this is the only allowed component within the Pickard-Mauri theory: it is easy to see that a purely tangential **A**-field yields a vanishing nonlocal contribution to the current [see Eq. (48)]. Then, the line integral needed for the first order term in Eq. (43) is

$$\begin{aligned}
\int_{\mathbf{s}'\to 0\to \mathbf{s}} \mathbf{A}\cdot d\ell &= A\left(\int_0^{\mathbf{s}} \hat{\mathbf{r}}_0 \delta(\mathbf{r}-\mathbf{r}_0)\cdot d\ell - \int_0^{\mathbf{s}'} \hat{\mathbf{r}}_0 \delta(\mathbf{r}-\mathbf{r}_0)\cdot d\ell\right) \\
&= A\left(\int_0^{\mathbf{s}} \frac{\delta(\hat{\mathbf{r}}-\hat{\mathbf{r}}_0)\delta(r-r_0)}{4\pi r^2}\cdot d\ell - \int_0^{\mathbf{s}'} \frac{\delta(\hat{\mathbf{r}}-\hat{\mathbf{r}}_0)\delta(r-r_0)}{4\pi r^2}\cdot d\ell\right) \\
&= \frac{A}{4\pi r_0^2}\left[\delta(\hat{\mathbf{s}}-\hat{\mathbf{r}}_0)\theta(s-r_0) - \delta(\hat{\mathbf{s}}'-\hat{\mathbf{r}}_0)\theta(s'-r_0)\right],
\end{aligned} \tag{E2}$$

where θ is the Heaviside step function, and, in the second line, we have rewritten the Dirac delta function in spherical coordinates. Therefore, we can write the current-density operator as

$$\langle \mathbf{s}|\hat{\mathcal{J}}(\mathbf{r})|\mathbf{s}'\rangle = \frac{iV^{\rm nl}(\mathbf{s},\mathbf{s}')}{4\pi r^2}\left[\delta(\hat{\mathbf{s}}-\hat{\mathbf{r}})\theta(s-r) - \delta(\hat{\mathbf{s}}'-\hat{\mathbf{r}})\theta(s'-r)\right]. \tag{E3}$$

Considering a general time-dependent wavefunction as in Eq. (8), the current density is

$$\begin{aligned}\mathbf{J}^{\rm nl}(\mathbf{r},t) &= \frac{i}{4\pi r^2}\int d^3s \int d^3s' \Psi^*(\mathbf{s},t)\Psi(\mathbf{s}',t)V^{\rm nl}(\mathbf{s},\mathbf{s}')\left[\delta(\hat{\mathbf{s}}-\hat{\mathbf{r}})\theta(s-r) - \delta(\hat{\mathbf{s}}'-\hat{\mathbf{r}})\theta(s'-r)\right] \\ &= \frac{i}{r^2}\sum_{lm}\int_r^\infty ds\left[\langle\phi_{lm}|\Psi(t)\rangle\Psi^*(s\hat{\mathbf{r}},t)\phi_{lm}(s\hat{\mathbf{r}}) - \langle\Psi(t)|\phi_{lm}\rangle\Psi(s\hat{\mathbf{r}},t)\phi^*_{lm}(s\hat{\mathbf{r}})\right]s^2 \\ &= -\frac{\hat{\mathbf{r}}}{r^2}\int_r^\infty ds\,\rho^{\rm nl}(s\hat{\mathbf{r}})s^2\end{aligned} \tag{E4}$$

where we have identified the nonlocal charge $\rho^{\rm nl}(\mathbf{r}) = -i\langle\Psi|\left[|\mathbf{r}\rangle\langle\mathbf{r}|,\hat{V}^{\rm nl}\right]|\Psi\rangle$ [*cf.* Eq. (32)]. Note that the upper limit of the integral can be set to $r_{\rm c}$, i.e., the core radius that was used in the generation of the pseudopotential (the nonlocal current density field is strictly contained within a sphere of radius $r_{\rm c}$). This shows that, in the special case of the Pickard-Mauri theory, the nonlocal density does, in fact, provide complete information about the current density.

Unfortunately, a consequence of the above derivations is that the nonlocal current density *diverges* as $|\mathbf{r}-\mathbf{R}|^{-2}$ in the vicinity of an atomic site $\mathbf{R}$. To see this it suffices to observe that the integral in the above equation tends, for $r\to 0$, to a direction-dependent constant,

$$\int_0^{+\infty} s^2 ds\,\rho^{\rm nl}(s\hat{\mathbf{r}}) = C(\hat{\mathbf{r}}). \tag{E5}$$

Thus, the current-density field diverges near the atomic site as

$$\mathbf{J}^{\rm nl}(\mathbf{r}) \sim \frac{\hat{\mathbf{r}}C(\hat{\mathbf{r}})}{r^2}. \tag{E6}$$

[1] M. S. Majdoub, R. Maranganti, and P. Sharma, Phys. Rev. B **79**, 115412 (2009).
[2] D. Lee, A. Yoon, S. Y. Jang, J.-G. Yoon, J.-S. Chung, M. Kim, J. F. Scott, and T. W. Noh, Phys. Rev. Lett. **107**, 057602 (2011).
[3] P. V. Yudin, A. K. Tagantsev, E. A. Eliseev, A. N. Morozovska, and N. Setter, Phys. Rev. B **86**, 134102 (2012).
[4] A. Y. Borisevich, E. Eliseev, A. Morozovska, C.-J. Cheng, J.-Y. Lin, Y.-H. Chu, D. Kan, I. Takeuchi, V. Nagarajan, and S. V. Kalinin, Nat. Commun. **3**, 775 (2012).
[5] G. Catalan, L. Sinnamon, and J. Gregg, J. Phys.: Conden. Mat. **16**, 2253 (2004).
[6] G. Catalan, B. Noheda, J. McAneney, L. J. Sinnamon, and J. M. Gregg, Phys. Rev. B **72**, 020102 (2005).
[7] H. Zhou, J. Hong, Y. Zhang, F. Li, Y. Pei, and D. Fang, Physica B: Condensed Matter **407**, 3377 (2012).
[8] A. N. Morozovska, E. A. Eliseev, M. D. Glinchuk, L.-Q. Chen, and V. Gopalan, Phys. Rev. B **85**, 094107 (2012).
[9] W. Zhu, J. Y. Fu, N. Li, and L. Cross, Applied Physics Letters **89**, 192904 (2006).
[10] U. K. Bhaskar, N. Banerjee, A. Abdollahi, Z. Wang, D. G. Schlom, G. Rijnders, and G. Catalan, Nat. Nanotechnol. **11**, 263 (2016).
[11] H. Lu, C.-W. Bark, D. Esque de los Ojos, J. Alcala, C. B. Eom, G. Catalan, and A. Gruverman, Science **336**, 59 (2012).
[12] A. Gruverman, B. J. Rodriguez, A. Kingon, R. Nemanich, A. Tagantsev, J. Cross, and M. Tsukada, Applied Physics Letters **83**, 728 (2003).
[13] P. Zubko, G. Catalan, and A. K. Tagantsev, Annual Review of Materials Research **43**, 387 (2013).
[14] P. V. Yudin and A. K. Tagantsev, Nanotechnology **24**, 432001 (2013).
[15] M. Stengel, Phys. Rev. B **88**, 174106 (2013).
[16] J. Hong and D. Vanderbilt, Phys. Rev. B **84**, 180101 (2011).
[17] J. Hong and D. Vanderbilt, Phys. Rev. B **88**, 174107 (2013).
[18] M. Stengel, Phys. Rev. B **90**, 201112 (2014).
[19] S. Baroni, S. de Gironcoli, A. Dal Corso, and P. Giannozzi, Rev. Mod. Phys. **73**, 515 (2001).
[20] M. Stegel and D. Vanderbilt, unpublished.
[21] R. D. King-Smith and D. Vanderbilt, Phys. Rev. B **47**, 1651 (1993).
[22] R. Resta, Rev. Mod. Phys. **66**, 899 (1994).
[23] J. Sakuri and J. Napolitano, *Modern Quantum Mechanics–*

2nd ed. (Addison-Wesley, San Fransisco, CA, 1994).
[24] C. Li, L. Wan, Y. Wei, and J. Wang, Nanotechnology **19**, 155401 (2008).
[25] D. Vanderbilt, Phys. Rev. B **41**, 7892 (1990).
[26] D. R. Hamann, M. Schlüter, and C. Chiang, Phys. Rev. Lett. **43**, 1494 (1979).
[27] L. Kleinman and D. M. Bylander, Phys. Rev. Lett. **48**, 1425 (1982).
[28] P. E. Blöchl, Phys. Rev. B **50**, 17953 (1994).
[29] P. Umari, A. D. Corso, and R. Resta, AIP Conference Proceedings **582**, 107 (2001).
[30] G. Vignale, Phys. Rev. Lett. **67**, 358 (1991).
[31] S. Ismail-Beigi, E. K. Chang, and S. G. Louie, Phys. Rev. Lett. **87**, 087402 (2001).
[32] C. J. Pickard and F. Mauri, Phys. Rev. Lett. **91**, 196401 (2003).
[33] F. Mauri and S. G. Louie, Phys. Rev. Lett. **76**, 4246 (1996).
[34] F. Mauri, B. G. Pfrommer, and S. G. Louie, Phys. Rev. Lett. **77**, 5300 (1996).
[35] C. J. Pickard and F. Mauri, Phys. Rev. B **63**, 245101 (2001).
[36] C. J. Pickard and F. Mauri, Phys. Rev. Lett. **88**, 086403 (2002).
[37] J. Nye, *Physical Properties of Crystals: Their Representation by Tensors and Matrices*, Oxford science publications (Clarendon Press, 1985).
[38] A. Messiah, *Quantum Mechanics, Vol. 2* (North-Holland, 1981) p. 752.
[39] D. J. Thouless, Phys. Rev. B **27**, 6083 (1983).
[40] Q. Niu and D. J. Thouless, J. Phys. A: Math. and Gen. **17**, 2453 (1984).
[41] M. V. Berry, P. Roy Soc. Lond. A Mat. **392**, 45 (1984).
[42] X. Gonze, Phys. Rev. B **55**, 10337 (1997).
[43] S. L. Adler, Phys. Rev. **126**, 413 (1962).
[44] Note that the definition of Eq. (23) involves a choice of convention in that the exponential factor $e^{i\mathbf{q}\cdot\mathbf{r}}$ is placed to the right of $\hat{\mathcal{J}}_\alpha(\mathbf{q})$ as opposed to the left. Choosing the opposite convention would simply switch the operators between the two terms in Eq. (24).
[45] A. F. Starace, Phys. Rev. A **3**, 1242 (1971).
[46] M. S. Hybertsen and S. G. Louie, Phys. Rev. B **35**, 5585 (1987).
[47] P. Giannozzi, S. de Gironcoli, P. Pavone, and S. Baroni, Phys. Rev. B **43**, 7231 (1991).
[48] A. Dal Corso, S. Baroni, and R. Resta, Phys. Rev. B **49**, 5323 (1994).
[49] A. M. Essin, A. M. Turner, J. E. Moore, and D. Vanderbilt, Phys. Rev. B **81**, 205104 (2010).
[50] In contrast to the ICL straight-line path, Eq. (42) using the PM $\mathbf{s}' \to \mathbf{R}_\zeta \to \mathbf{s}$ path [i.e., the phase in Eq. (48) multiplying the entire Hamiltonian instead of just $V^{\rm nl}(\mathbf{s},\mathbf{s}')$] does *not* recover $\hat{\mathcal{J}}^{\rm loc}_\alpha$ for local potentials.
[51] R. M. Martin, Phys. Rev. B **5**, 1607 (1972).
[52] D. Vanderbilt, J. Phys. Chem. Sol. **61**, 147 (2000).
[53] M. Stengel, Nat. Commun. **4**, 2693 (2013).
[54] M. Stengel and D. Vanderbilt, in *Flexoelectricity in Solids From Theory to Applications*, edited by A. K. Tagantsev and P. V. Yudin (World Scientific Publishing Co., Singapore, 2016) Chap. 2, pp. 31–110.
[55] X. Gonze, B. Amadon, P.-M. Anglade, J.-M. Beuken, F. Bottin, P. Boulanger, F. Bruneval, D. Caliste, R. Caracas, M. Ct, T. Deutsch, L. Genovese, P. Ghosez, M. Giantomassi, S. Goedecker, D. Hamann, P. Hermet, F. Jollet, G. Jomard, S. Leroux, M. Mancini, S. Mazevet, M. Oliveira, G. Onida, Y. Pouillon, T. Rangel, G.-M. Rignanese, D. Sangalli, R. Shaltaf, M. Torrent, M. Verstraete, G. Zerah, and J. Zwanziger, Computer Physics Communications **180**, 2582 (2009).
[56] J. P. Perdew, K. Burke, and M. Ernzerhof, Phys. Rev. Lett. **77**, 3865 (1996).
[57] X. Gonze, Phys. Rev. B **55**, 10337 (1997).
[58] X. Gonze and C. Lee, Phys. Rev. B **55**, 10355 (1997).
[59] D. R. Hamann, Phys. Rev. B **88**, 085117 (2013).
[60] H. J. Monkhorst and J. D. Pack, Phys. Rev. B **13**, 5188 (1976).
[61] R. M. Pick, M. H. Cohen, and R. M. Martin, Phys. Rev. B **1**, 910 (1970).
[62] H. P. R. Frederikse and G. A. Candela, Phys. Rev. **147**, 583 (1966).
[63] This can be deduced from Eq.(12) and (13) of Ref. 32: By placing a single spherical pseudoatom in the gauge origin, all nonlocal contributions vanish by construction as they are multiplied by $\mathbf{R}$; thus, the applied magnetic field enters the Hamiltonian via the usual substitution $\mathbf{p} \to \mathbf{p}+\mathbf{A}$. Then, the first order Hamiltonian is the angular momentum operator, which commutes with the ground-state density matrix and yields a vanishing linear response, and the second-order piece picks the quadrupolar moment of the ground-state density, as in the local case.
[64] F. S. Khan and P. B. Allen, Phys. Rev. B **29**, 3341 (1984).
[65] R. M. Martin, *Electronic structure: basic theory and practical methods* (Cambridge university press, 2004).